

**IMMUNE RESPONSES IMPORTANT IN THE REGULATION OF HUMAN IMMUNODEFICIENCY
VIRUS-1 (HIV-1) AND HEPATITIS C VIRUS (HCV) IN PEOPLE WHO INJECT DRUGS (PWID)**

by
Mary George Soliman

A dissertation submitted to Johns Hopkins University in conformity with the requirements for
the degree of Doctor of Philosophy

Baltimore, Maryland
August 2020

© 2020 Mary Soliman
All rights reserved

Abstract

Increased mortality among people who inject drugs (PWIDs) is attributed in part to the higher prevalence of chronic viral infections, notably HIV-1 and HCV. Approximately 38 million people globally are currently living with HIV-1. Type 1 interferons are important host factors that respond to HIV-1 infection by upregulating many interferon-stimulated genes (ISGs) with diverse antiviral effects. ISGs that restrict HIV-1 in humans have been poorly characterized; however, they demonstrate potential to be small molecule inhibitors that target HIV-1 during various stages in the life cycle. Here, we aim to better understand ISGs important in controlling HIV-1 infection. Therefore, we enrolled 19 HIV-1 infected patients with uncontrolled viremia and administered peginterferon alpha 2b (IFN). RNAseq was performed on activated CD4+ T cells and ISGs up-regulated in at least 11/19 people were identified. Both BCL2L14 and CMPK2 were identified as ISGs that were important in controlling HIV-1 in this cohort. RNA interference demonstrated that the anti-HIV-1 effect of IFN α could be attributable to both CMPK2 and BCL2L14. This is the first study to comprehensively assess both CMPK2 and BCL2L14 role's in HIV-1 infection.

Hepatitis C virus (HCV) remains another major global health epidemic, with approximately 70 million infected worldwide. Approximately 25% of individuals infected with HCV spontaneously clear infection. These individuals mount responses that lead to subsequent control of future HCV infections. Although the ability to spontaneously control multiple HCV infections is not indicative of sterilizing immunity, it seems to provide protective immunity against future

reinfections. Here, we aim to better understand HCV- specific CD8+ and CD4+ T-cells by developing a high-parameter phenotypic flow cytometry panel. This panel will simultaneously assess 27 phenotypic markers, including many exhaustion markers, to fully characterize CD4+ and CD8+ T-cells in individuals who progress to chronic infection, in comparison to those who spontaneously clear multiple reinfections. This work aims to inform vaccine development by characterizing essential cytolytic T-cell (CTL) epitopes for controlling infection, identifying inhibitory marker/s, and characterizing rare T-cell populations that may be important in controlling HCV infection. Most importantly, this work is the first development of a high parameter flow cytometry panel to study HCV- specific T-cells in reinfection.

Advisors:

Dr. Andrea L. Cox and Dr. Ashwin Balagopal (Readers)

Thesis Committee:

Dr. Robert F. Siliciano (Chair)

Dr. Joel N. Blankson (Reader)

Dr. Justin R. Bailey

Acknowledgements

I would like to thank both my mentors Dr. Andrea L. Cox and Dr. Ashwin Balagopal for supporting me through graduate school career. Andrea has always served as a role model of women in science, eloquently balancing brilliance and compassion. She never left a meeting without asking me about my well-being, and for that, I will always be grateful. Ashwin's positive outlook and constant support when I was struggling through my experiments, taught me the important life lesson of resilience. I was very lucky to have both of them as mentors. I would especially like to thank Dr. Joel N. Blankson for not only being a scientific mentor, but a life mentor. He was a major player in my well-being throughout graduate school. I would also like to thank Dr. David Thomas for his insightful advice when troubleshooting experiments, and for supporting me through graduate school. In addition, I appreciate the support of Dr. Eileen Scully and Dr. Justin Bailey for providing new ideas and techniques to advance my project. My success in lab was attributed to my wonderful lab mates and Dr. Ramy El-Diwany. I would also like to thank the CMM graduate training program including Dr. Rajini Rao, Colleen Graham, and Leslie Lichter. I appreciate the training from many individuals in the Vaccine Research Center at the NIH, and more specifically, Matthew Sutton.

Lastly, I would love to thank my wonderful family for understanding the sacrifices I had to make in graduate school. They were always encouraging and cheering me on during some of the most stressful times. More specifically, thank you to my wonderful younger brother Cyril Soliman for all the late-night pep talks. I would like to thank my CMM classmates for giving me the best cohort to have alongside this graduate school journey. To all the wonderful security guards, delivery personal, and janitorial staff that constantly put a smile on my face, I thank

you. To all the wonderful friends I made in Baltimore through my church community and gym community, I will never forget all the encouragement you gave me to push through all obstacles.

TABLE OF CONTENTS

ABSTRACT	ii
ACKNOWLEDGEMENTS	iv
LIST OF TABLES	vii
LIST OF FIGURES	viii
CHAPTER I: Introduction	1
CHAPTER II: Identification of CMPK2 and BCL-G as Interferon Stimulated Genes that Restrict HIV-1 Infection	21
ABSTRACT.....	22
INTRODUCTION	23
METHODS	24
RESULTS	28
DISCUSSION/LIMITATIONS.....	32
FIGURES.....	36
CHAPTER III: High-dimensional flow cytometry analysis of T-cell responses in individuals who clear multiple reinfections versus remain persistently infected with HCV	50
ABSTRACT.....	51
INTRODUCTION	51
METHODS	52
RESULTS	55
DISCUSSION/LIMITATIONS.....	58
TABLES	61
FIGURES.....	63
CHAPTER IV: Conclusions	71
REFERENCES	74
CURRICULUM VITAE FOR Ph.D. CANDIDATES	98

LIST OF TABLES

Table 1.1 Mechanisms of HIV-1 evasion.....	20
Table 3.1 The Optimized 27-color Panel for Flow Cytometry.....	61
Table 3.2 Summary of Subjects and Pentamer Sequence Used for Flow Cytometry	62

LIST OF FIGURES

Figure 1.1: Inhibition of HIV replication by known host restriction factors.....	18
Figure 2.1A: CMPK2 and MX2 proteins are induced by IFN in THP-1 and MT4 cells.....	36
Figure 2.1B: Restriction of HIV in vitro is dependent on the IFN induction of CMPK2.....	36
Figure 2.1C: CMPK2 knockdown using siRNA in THP-1 cells.....	37
Figure 2.2A: Overexpression minimally inhibits HIV infection on CCR5-U87 cell.....	38
Figure 2.2B: Overexpression of BCL-G-myc does not inhibit HIV RNA.....	38
Figure 2.2C: Overexpression of BCL-G-myc does not inhibit production of first (minus) strand cDNA.....	39
Figure 2.3A: BCL-G overexpression in 293T/17 cells causes degradation of BCL-G.....	40
Figure 2.3B: MG132 treatment minimally rescues the degradation of BCL-G.....	40
Figure 2.3C: Co-expression of BCL-G with BCL-XL causes an increase in protein levels of BCL-G and its degradation products.....	41
Figure 2.4A: Correlation plots of the top ten statistically significant genes.....	42
Figure 2.4B: The top 50 correlated gene with BCL-G Pre-IFN.....	43
Figure 2.4C: Pairwise Correlation Plots for the top correlated genes Pre-IFN.....	43
Figure 2.4D: Principle Component Analysis of the top 50 genes Pre-IFN.....	44
Figure 2.4E: Pairwise Correlation Plots for the top correlated genes Post-IFN.....	45
Figure 2.4F: Pairwise Correlation Plots for the top correlated genes Post-ART.....	46
Figure 3.1A: N by N plot of All Markers in 27-Color Flow Panel.....	63
Figure 3.2: Representative graphs demonstrating the longitudinal history of viremia in subjects S29 and S553.....	64
Figure 3.3: Staining Pattern for gating, T-cell differentiation characterization, and identifying HCV-specific CD8+ T-cells.....	65

Figure 3.4: High dimensional analysis of HCV-Specific CD8+ T-cells in S29 and S553.....	66
Figure 3.5: HCV-specific CD8+ T-cells diverge in phenotype in S29 and S553.....	67
Supplementary Figure 2.1: IFN-mediated restriction of HIV-1 in various cell lines.....	47
Supplementary Figure 2.2: IFN restriction of HIV-1 in THP-1 cells is dependent on CMPK2	47
Supplementary Figure 2.3: Overexpression of myc-tagged BCL-G in CCR5-U87 cells causes degradation.....	48
Supplementary Figure 2.4: Heatmap Analysis of Top fifty genes Pre-IFN.....	49
Supplementary Figure 3.1: Titration of CD3 and CD4 for the 27-color Flow Panel.....	68
Supplementary Figure 3.2: HCV-Specific CD8+ T-cells in S29 and S553.....	69
Supplementary Figure 3.3: Median MFI of TIM-3, KLRG1, and LAG3 in S29 and S553.....	69
Supplementary Figure 3.4: HCV-specific CD8+ T-cell phenotype in S29 and S553.....	70

Chapter I

Introduction

Soliman M, Srikrishna G, Balagopal A. Mechanisms of HIV-1 Control. *Curr HIV/AIDS Rep.* 2017;14(3):101-109. doi:10.1007/s11904-017-0357-9.

Mechanisms of HIV Control

Introduction

HIV-1 infects 37 million people worldwide, killing roughly 1 million people per year. Life-saving antiretroviral therapy controls, but does not eliminate, the virus. Whereas an HIV-1 cure is necessary, a clearer understanding of the intracellular fate(s) of HIV-1 is essential before a potent cure can be designed. Indeed, the host cell has several mechanisms by which it can limit replication of HIV-1, and an elucidation of these mechanisms offers keen insights into HIV-1 biology. In that context, we have reviewed recent advances describing intracellular genes that restrict HIV-1.

Innate Immunity: sensing and restriction

Innate immunity has received considerable attention recently for its role in host defense and inflammation. As a simplification, shared molecular patterns on invading pathogens can be recognized by intracellular sensors, triggering a downstream cascade of gene regulation in processes that have been extensively reviewed elsewhere [1, 2]. Many of the upregulated genes in innate immune cascades are devoted to ridding the host cell of the pathogen and/or recruiting a targeted adaptive response. With viruses, viral nucleic acids and structural components are often recognized by pattern recognition receptors, whereas downstream antiviral effector molecules target replication within the cell [3-5]. A hallmark example of an innate immune pathway with potent antiviral effects is the type 1 interferon pathway: upon sensing of viral nucleic acids, type 1 interferons are released. These in turn trigger the

transcription of hundreds of genes termed interferon-stimulated genes (ISGs), many of which directly constrain viral replication [6].

HIV-1 is a retrovirus: productive infection of host cells requires that uncoated HIV-1 RNA is reverse transcribed into a DNA provirus that is then integrated into the host cell's genome.

Conceptually, we have divided our review into restriction that occurs prior to HIV-1 integration and restriction that occurs post-integration (**Figure 1.1**). This conceptual division is to stress that pre-integration restriction necessarily occurs in cells that are not yet infected, whereas restriction post-integration occurs in cells that are already infected. We have also described the key adaptive measures that have evolved in HIV-1 to overcome restriction (**Table 1.1**).

IFITM

The interferon-induced transmembrane gene family (IFITM), comprising IFITM1, IFITM2, and IFITM3, restrict a broad panoply of viruses from entering the host cell [7]. The IFITM family are ISGs. IFITM1 was the first in this group to be discovered in an RNA silencing screen of ISGs that conferred resistance to Influenza A, West Nile, and dengue viruses [8]. IFITM1 is mostly found on the plasma membrane and has a role in blocking entry of HIV-1 virions [9]. In contrast, IFITM2 and -3 are largely localized to the late endosome and lysosomes [10, 11]. The IFITM genes are thought to inhibit HIV-1 entry by changing the composition and curvature of the plasma membrane, perhaps reducing its fluidity, thereby interfering with a phenomenon known as hemifusion [12, 13]. Hemifusion is essential for the incorporation of an HIV-1 virion into a target cell [14]. Intriguingly, although restriction of HIV-1 entry occurs pre-integration, there are two reports suggesting a role post-integration: Compton et al. found that the presence of IFITM3 in HIV-1 infected cells decreased transmission of HIV-1 to target cells [15]. Moreover,

time-lapse microscopy has shown that IFITM3 functions by decreasing fusion between the infected and uninfected target cell by affecting the virus membrane. Yu et al. confirmed that IFITMs were incorporated into HIV-1 virions and interacted with the envelope protein Env to restrict HIV-1 infection [16].

There is evidence that certain HIV-1 variants may be resistant to the restriction of IFITM proteins. In particular, transmitter/founder viruses have been found to be more resistant to IFITM restriction than viruses isolated from later times during infection; the later viruses may gain sensitivity as a result of escape from concomitant neutralizing antibody responses [17], although this in turn raises the question as to the relative relevance of IFITM as an *in vivo* restriction mechanism compared to antibody-driven selection.

TRIM5 α and TRIM22

Tripartite motif 5 α (TRIM5 α), the longest splicing isoform of TRIM5 gene, was identified as a key molecule in old world monkeys that confers potent resistance against HIV-1 [18]. Among the large family of TRIM proteins consisting of over 70 family members in the human genome, TRIM5, TRIM11, TRIM15, TRIM19, TRIM22, TRIM28, and TRIM31 all have been described as having antiretroviral activity, although the human TRIM5 α only confers modest resistance to HIV-1 [19-22]. It is thought, then, that TRIM proteins are required to prevent cross-species transmission of retroviruses [23].

TRIM proteins are multi-domain proteins defined by an N-terminal RING finger with E3 Ubiquitin ligase activity, one or two B-box domain(s), and a coiled-coil (RBCC) domain [19]. Some of the TRIM genes, including TRIM5 α , also possess a C-terminal PRY/SPRY (SPLa and the

RYanodine Receptor) domain that is important for HIV-1 capsid recognition [24]. TRIM5 α acts at multiple levels to restrict HIV-1 replication. It specifically binds the capsid (CA) lattice of HIV-1 and induces premature disassembly of viral particles, accompanied by proteosomal-degradation of viral components such as integrase [25]. TRIM5 α has also been found to promote autophagic degradation of retroviruses by interacting with Atg8 proteins [26]. More recent studies show that TRIM5 α inhibits HIV-1 infection by sensing the retrovirus capsid lattice, eliciting an innate immune response [27]. Interaction with the capsid lattice enhances TRIM5 α RING-associated E3-Ub ligase, which in turn promotes the synthesis of free Lys63-linked Ub chains that bind to the TAK1 kinase complex. TAK1 ubiquitination leads to nuclear translocation of the transcription factors NF- κ B and AP-1 that result in type 1 IFN and other pro-inflammatory cytokines [28] [29], broadly inducing an antiviral state.

Whereas the TRIM5 α homolog in humans does not inhibit HIV-1 well, TRIM22, a human paralog of TRIM5 α , is involved in type I IFN-mediated restriction of HIV-1 replication [30, 31]. TRIM22 inhibits HIV-1 replication by interfering with Tat- and NF- κ B-independent LTR-driven transcription, and by preventing Sp1 binding to the HIV-1 promoter [32, 33]. TRIM22 may also interfere with virion assembly and release by preventing the trafficking and budding of Gag proteins and Gag-containing virus particles [30].

Notably, because human TRIM5 α has only modest activity against HIV-1, it does not drive adaptation in the virus. However, several reports have suggested that HIV-1 could acquire adaptive mutations in the capsid gene, among others, in the setting of an engineered TRIM5 α molecule that did have the capacity to restrict HIV-1 replication [34] [35].

SAMHD1

SAMHD1 (Sterile alpha motif and histidine-aspartate domain containing protein 1) was discovered in 2011 as a restriction factor by two independent groups using a mass spectrometry pull-down approach to identify proteins that co-immunoprecipitated with the viral protein x (Vpx) present in HIV-2, but not HIV-1 [36, 37]. SAMHD1 is expressed at high levels in myeloid-derived cells and in resting CD4⁺ T cells that are refractory to HIV-1 infection [36, 38, 39]. However, SAMHD1 is inducible by type I IFN in monocytes, but not in dendritic cells or resting CD4⁺ T cells [40]. SAMHD1 comprises three regions, the N-terminus sterile alpha motif (residues 1–109), a catalytic histidine aspartate core domain (residues 110–599), and the C-terminus (residues 600–626) [41]. The catalytic core domain has 2'-deoxynucleoside 5'-triphosphate triphosphohydrolase (dNTPase) activity that is believed to restrict HIV-1 by diminishing the intracellular pool of available dNTP in immune cells needed for cDNA synthesis during reverse transcription [42-44]. The anti-HIV-1 activity of SAMHD1 is negatively modulated by phosphorylation at residue Thr-592, and the phosphomimetic mutation T592E impairs dNTPase activity [45]. Indeed, dNTP levels are elevated in SAMHD1-deficient cells, whereas reduced dNTPs lead to an attenuation of reverse transcription [46-48].

Another feature of human SAMHD1 is that it exhibits metal-dependent 3'→5' exonuclease activity against single-stranded DNAs and RNAs *in vitro*, suggesting that it may bind to and degrade HIV-1 RNA [49]. Ryoo and colleagues created several SAMHD1 mutants that exclusively retained either their exonuclease activity or their dNTPase activity and showed that the exonuclease alone was sufficient to partially restrict HIV-1 [50].

Restriction is overcome by Vpx in HIV-2 through interactions with the host Ub ligase adaptor DCAF1 that promotes SAMHD1 degradation [36, 37]. Whether HIV-1 has evolved adaptations to

counter SAMHD1 is still not well understood, although recently Kyei et al. reported that HIV-1 might neutralize SAMHD1 in macrophages in concert with the cell cycle regulator cyclin L2 [51]. There is suggestive evidence for the clinical relevance of SAMHD1: the gene is mutated in a subset of patients suffering from Aicardi-Goutières syndrome (AGS), and monocytes from patients with AGS appear exquisitely susceptible to HIV-1 infection, in contrast to monocytes from healthy persons [52].

APOBEC3

Apolipoprotein B editing complex 3 (APOBEC3) family members are cytidine deaminases that include APOBEC3A-H [53, 54]. They are induced by Type I IFN and most play important roles in control of multiple retroviruses through RNA binding or through deamination of single-stranded DNA (ssDNA) [53]. APOBEC3 proteins are expressed variably in CD4⁺ and CD8⁺ T cell subsets, B cells, and myeloid cells [55]. APOBEC3G exerts a dominant antiviral effect in CD4⁺ T cell subsets [56], and in macrophages and primary CD4⁺ T cells shows more potent restriction of HIV-1 than the combined effect of APOBEC3F and APOBEC3DE [57]. The APOBEC3 family members restrict HIV-1 by hypermutating its genome, resulting in premature stop codons and defective proviruses that are incapable of propagating infection [58, 59]. APOBEC3G, for example, acts by temporarily inhibiting the reverse transcription step and deaminating C→U on the minus strand of the DNA, leading to a mismatch pairing of a G→A on the plus strand, thus causing genomic mutations [60]. Hypermutation leads to HIV-1 restriction in at least two ways: i) the host cell recognizes ssDNA as aberrant and degrades it [61]; and ii) proviral DNA is integrated as a defective provirus that is no longer capable of producing infectious virions, usually due to premature stop codons [62]. The restrictive activity of APOBEC3G depends on its encapsidation

in the budding virion, mediated by the nucleocapsid domain of Gag molecules: upon virion fusion with a target cell, the viral RNA, reverse transcriptase, integrase, and APOBEC3G are released into the cytosol, allowing restriction to occur in the target cell [63, 64]. In addition, APOBEC3F and -G may exert antiretroviral activities that are independent of their deaminase functions by interfering with reverse transcription, either terminating the synthesis of the minus-strand or preventing tRNA molecules from binding HIV-1 nucleic acids.

HIV-1 has developed a significant adaptation to APOBEC3 restriction: the accessory protein Vif triggers the degradation of APOBEC3 proteins through polyubiquitination and proteasomal degradation [65-67]. Ubiquitination occurs by the recruitment of a Cullin 5-based E3 ubiquitin ligase complex consisting of elongin B, elongin C, and Rbx-1. The *in vivo* relevance of APOBEC3G is evident in recent reports showing that the HIV-1 latent reservoir in patients treated with antiretrovirals contains a large number of APOBEC3G hypermutated sequences [68, 69, 65]. Collectively, human studies suggest that the battle between HIV-1 and APOBEC3 is not concluded. Whereas the latent reservoir is largely defective, there exist replication competent viruses that impede an HIV-1 cure. Similarly, Vif efficiently blocks APOBEC3 genes, but is insufficient in terminating all hypermutation. The latter point is promising for strategies aimed at enhancing inactivation of proviruses.

MX2

The IFN-inducible myxovirus resistance 2 (MX2/MXB) is a member of a family of dynamin-like GTPases that includes human MX1/MXA, another well-known IFN-inducible inhibitor of a broad range of viruses. In 2013, the anti-HIV-1 activity of MX2 was described by three separate groups [70-72]. MX2 appears to act at a late post-entry step prior to integration of proviral DNA,

possibly through inhibition of nuclear import following reverse transcription, or by inhibiting the uncoating of HIV-1 [70, 71, 73]. It has also been proposed that MX2 could decrease integration of nascent viral DNA, leading to nuclear accumulation of 2' LTR circles [70]. MX2 interacts with the HIV-1 capsid and may be dependent on CypA: substitutions in the CypA binding loop at positions 86-88 and 92 disrupt the binding of MX2 and capsid protein [74]. Similarly, treatment with cyclosporine, which blocks the CypA interaction with capsid, reduces the restrictive ability of MX2 [72].

There is little *in vivo* data to support the relevance of MX2 in HIV-1 restriction, although our group has found strong evidence that interferon administration to HIV-1 infected persons led to MX2 induction and proportional declines in plasma HIV-1 RNA in activated CD4+ T cells. In addition, mutations in the HIV-1 capsid protein and in integrase confer resistance to MX2 [75]. It is yet to be understood how the potency of MX2 compares with other interferon-inducible HIV-1 restriction factors in humans.

SLFN11

SLFN11 belongs to the Schlafen family of mouse and human proteins implicated in the control of cell proliferation, immune responses, and the regulation of viral replication [76]. It has recently been identified as inducible by type 1 IFNs [77]. SLFN11 does not inhibit reverse transcription, DNA integration, production and nuclear export of viral RNA, or budding or release of viral particles. Its role in inhibition is one of the first to be associated with codon bias, inhibiting the expression of viral proteins. It binds to tRNAs, limiting their availability, thereby leading to a decrease in protein synthesis [77]. SLFN11 was also recently found to be significantly elevated in CD4+ T cells from elite HIV controllers as compared to non-controllers

and ART-suppressed individuals, suggesting that SLFN11 may play a role in the suppression of HIV-1 *in vivo* [78]. However, it is not clear whether the effects of SLFN11 are sufficiently robust to promote adaptation in HIV-1 *in vivo*.

MARCH8

Recently, Tada *et al.* reported that the membrane-associated RING-CH8 (MARCH8) E3 ubiquitin ligase, a gene that is highly expressed in terminally differentiated myeloid cells such as macrophages and dendritic cells, possesses potent anti-HIV-1 activity *in vitro* [79]. The antiviral effect of MARCH8 was discovered serendipitously when the investigators noted that the transduction efficiency of lentiviruses produced from MARCH8-expressing cells was several-fold lower than that of control lentiviruses. MARCH8 blocks the incorporation of HIV-1 envelope glycoprotein into virus particles, resulting in a substantial reduction in the efficiency of virus entry, thus inhibiting its infectivity. Intriguingly, viruses are normally released, but are rendered non-infectious in the presence of MARCH8. Neither HIV-1 Vpr, Vpu nor Nef have detectable anti-MARCH8 activity, suggesting that HIV-1 lacks a counter-mechanism that dampens the effects of MARCH8. Studies are ongoing to determine the *in vivo* relevance of MARCH8, and whether HIV-1 can indeed adapt resistance to its effects.

Tetherin

Tetherin (Bone marrow stromal cell antigen-2 [BST-2]; CD317) is a restriction factor that was first identified in a microarray screen aimed at finding ISGs that are associated with the plasma membrane in cells that were not permissive for HIV-1 propagation [80]. Tetherin consists of an N-terminal cytoplasmic tail, a transmembrane helix, a coiled-coil ectodomain, and a C-terminal

glycosylphosphatidylinositol (GPI) membrane anchor. It is localized in lipid rafts at the plasma membrane, in the trans-Golgi network, and in early recycling endosomes [81]. Tetherin inhibits the release of nascent HIV-1 particles by tethering the budding virions at the cell surface [82]. Nascent virions anchored to the membrane are then internalized and degraded in the lysosome. Interestingly, the topology of tetherin is unique. When a mimic of tetherin was designed from unrelated proteins, HIV-1 was inhibited, demonstrating that the topology of tetherin, not the sequence, is key to its restrictive function.

Another proposed role of tetherin in infection is its role as a viral sensor. It has been suggested that a budding virion could act as a pathogen-associated molecular pattern that is sensed by tetherin. As tetherin binds budding virions, clustering of tetherin dimers promotes the recruitment of TRAF2 and TRAF6, leading to activation of TAK1 and NF- κ B and upregulation of proinflammatory cytokines such as CXCL10, IL-6 and IFN-gamma [83, 84]. The ability of tetherin to activate NF- κ B requires multimerization [83].

HIV-1 has evolved several viral proteins have evolved to antagonize tetherin: HIV-1 Vpu (in groups M and N) and Nef (in group O) [85, 80, 86]. Indeed, the role of tetherin as a broad antiretroviral is evident in that HIV-2 and SIV have evolved resistance to their host versions of tetherin [87]. HIV-1 Vpu, a small transmembrane protein, interacts directly with tetherin at the trans-Golgi network and targets it for proteasomal or lysosomal degradation [88, 89]. Deletion of Vpu results in tetherin-mediated retention of virions at the plasma membrane [80]. In addition, Vpu also inhibits the activation of NF- κ B by tetherin [84].

SERINC3/5

In a study structured to find constitutively expressed restriction factors that are suppressed by Nef, Usami *et al.*, discovered that SERINC3 and SERINC5 were both able to restrict HIV-1 replication [90]. In Nef-deleted HIV-1 pseudotyped virus, the addition of SERINC5 significantly reduced infectivity. The amount of SERINC5 expression was directly associated with a quantitative loss of fusion of HIV-1 Δ nef virions when co-expressed with a chimeric B-lactamase-Vpr. To further support these effects, SERINC5 mRNA level was inversely correlated with a requirement of Nef for HIV-1 replication in several cell lines (Jurkat, 293T, MT4).

SERINCs are cell surface proteins that function by incorporating serine into membrane lipids, most notably in sphingolipids and phosphatidylserine [91]. The lipid composition of the viral envelope is important for infectivity. Furthermore, SERINC5 inhibits the completion of reverse transcription of HIV-1 in the absence of Nef, which is an essential step prior to provirus integration [90]. Although the importance of SERINC3/5 can be inferred from their inhibition by Nef, more work is needed to understand the clinical relevance of these genes in HIV-1 infected persons.

Clinical Implications of HIV-1 Restriction Factors

Studies of restriction factors offer insights into the key molecular determinants of HIV-1 replication, and collectively outline a roadmap of HIV-1 vulnerabilities that could be targeted therapeutically. As an example, interferon alpha has been used to non-specifically target HIV-1 in several small trials of HIV-1 infected persons, and has been as effective as a single, modestly active antiretroviral drug [92]. Presumably, the actions of interferon alpha are at least partially in inducing ISGs that directly act on HIV-1 in the cells that are most susceptible to infection, but it is certainly possible that interferon alpha also recruits cellular immune responses. Although

interferon alpha may not add benefit to HIV-1 infected patients because of its side effects, it is compelling to consider that genes and pathways downstream of interferon administration may be specifically targeted to produce similar effects on HIV-1 replication. We speculate that for HIV-1 infected patients who have suppressed viral replication with antiretrovirals, it may be possible to silence integrated proviruses by exploiting or mimicking the actions of post-integration restriction factors.

Another approach to HIV-1 treatment follows from its adaptation to host restriction factors by the use of accessory proteins. Since these genes appear to be essential for the virus to circumvent host innate immunity, enzymatic inhibition of the activities of these accessory proteins may restore the ability of the host to control HIV-1 using its suite of restriction factors. Indeed, there has been a push of small molecules into clinical trials that have been demonstrated to have high potency activity against HIV-1 accessory proteins [93,94].

Conclusion

To address the challenge of an HIV-1 cure, a better understanding is required of how HIV-1 persists despite host cell restriction. Presently, the science of restriction factors is moving from the bench to the bedside as we explore which restriction factors are active in HIV-1 infected persons, and what measures can be used to enhance restriction. Future HIV-1 cure trials may indeed exploit HIV-1 restriction or, alternatively, target the adaptive means by which HIV-1 evades restriction.

Mechanisms of Control in HCV

The need for a HCV prophylactic vaccine despite recent development of Directly Acting Antivirals

Hepatitis C virus (HCV) infection is an important global health crisis, with approximately 70 million people infected worldwide [95]. During acute infection, many individuals remain asymptomatic and the long-term outcome of infection is determined. In the United States, only 50% of individuals are aware of their HCV status and are, therefore, at risk for disease progression due to untreated chronic HCV infection. Chronic infection can lead to liver cirrhosis and hepatocellular carcinoma [96-97]. In efforts to combat the rising rate of HCV-associated liver disease, directly acting antivirals (DAAs) were developed and cure HCV infection in the majority of treated patients. However, eradication by DAAs is limited due to cost, the asymptomatic nature of HCV infection that leaves infected people unaware, reinfection after treatment, and limited treatment uptake in individuals who are most at risk of infection (people who inject drugs, PWID) [98]. Despite the ability of DAAs to cure HCV, they do not protect against future reinfections or completely reverse disease for individuals with advanced liver disease. These limitations demonstrate the importance of developing a HCV prophylactic vaccine.

Understanding natural infection of HCV and induction of protective immunity

Chronic infection is established in 75% of individuals who are infected with HCV, while the other 25% naturally clear the virus [98]. Spontaneous clearance of the primary infection doesn't

provide sterilizing immunity against subsequent infection, but it does provide protective immunity. Humans who spontaneously clear the first infection clear 83% of reinfections [99]. Subsequent HCV infections are generally characterized by lower peak viral titers, with shorter duration of viremia until clearance compared to the primary infection [99]. Viral challenge studies in chimpanzees demonstrated similar low titers and decrease in duration of viremia with both homologous and heterologous viral challenges [100]. The control of reinfections in humans have been associated with cellular responses and development of broadly neutralizing antibodies [99].

Evidence for Cellular responses in controlling HCV infection

Characterization of cellular immune responses that distinguish chronic infection from spontaneous clearance are still poorly understood. Previous studies have shown that induction of broad and robust cellular immune responses is associated with spontaneous clearance [100-103], in contrast to the low frequencies of HCV-specific CD8+ T-cells in those that remain chronically infected [104-109]. CD8+ T-cells are essential for the control of infection with a clear association between control of viremia and development of HCV-specific CD8+ T-cells [110-111]. Durable CD4+ T-cell responses develop in individuals who spontaneously clear, although they develop in chronically infected individuals as well. Both CD4+ T-cell and CD8+ T-cell responses arise early infection regardless of outcome of infection, and may even persist during chronic infection; however, cellular responses are characterized as defective early in infection in those that persist [112]. Studies have demonstrated that in the chronic phase of infection, there was a gradual loss in both breadth and magnitude of cellular responses [113]. In

persistent infection, development of new epitope specificities after the first six months of infection were no longer seen. Altogether, this suggests the development of cellular responses is arrested within the first year of infection.

Cellular Immune Responses in Reinfected Individuals

The viral kinetics of reinfected subjects differ from those who progress to chronic infection. With exposure of new viruses, new T-cell responses were detected in all reinfected individuals, compared to one out of 12 subjects who progressed to chronicity. These data suggest that initial control of viremia is essential to generating new cellular immune responses, and not infection with new genotypically unique virus [113]. However, despite generation of new cellular responses in reinfected subjects, absolute protection was not guaranteed, as seen in some subjects that become persistently infected after initial control of viremia.

Evasion of Cellular Responses mounted Against HCV by sequence variation

HCV is highly variable and the quasispecies of variants differ from person to person. This can be attributed to the high level of virion turnover and the error prone HCV RNA polymerase, resulting in frequent mutations [114]. Studies have shown that CD8+ T cell escape early in infection plays a role in determining outcome, due to the low rate of amino acid substitutions seen early during longitudinal studies [115, 123]. The generation of mutations can have a deleterious, neutral, or advantageous effect on the virus by promoting evasion of cellular immune responses. It has been reported that in persistent infection there was a 16.7-fold higher likelihood of mutations within a T cell epitope compared to outside [113]. This evasion of

immune responses by mutating within the T-cell epitopes has negative effects for the host by decreasing MHC binding, impairing antigen processing or presentation, and affecting T-cell receptor engagement [116-123].

Other mechanisms of Evasion of Cellular Responses mounted Against HCV

T- cell inhibitory receptors are increasing in importance in eliciting effector function in both CD8+ and CD4+ T-cells. One inhibitory marker of importance is programmed death-1 (PD-1). PD-1 surface levels are higher on HCV-specific T-cells in both the acute and chronic phase of individuals who fail to control HCV [113]. PD-1 levels on HCV-specific T-cells correlate with HCV RNA levels, and is also associated with progression to chronicity, independent of HCV RNA levels [124]. Upregulation of PD-1 in HCV infection is dependent on both the presence of pro-inflammatory signals upon TCR engagement, and the presence of intact antigen [125-126]. Despite PD-1's association with HCV RNA levels, data have shown that expression on HCV antigen-specific T-cells during the chronic phase greatly varied. In some cases, PD-1 levels remained low despite high viral titers during the chronic phase of infection. This low expression of PD-1 was associated with escape mutations in the T-cell epitope. PD-1 levels remained high on all T-cells with intact antigen, and mutated T-cell epitopes expressed high levels of PD-1 when the intact antigen was restored [127].

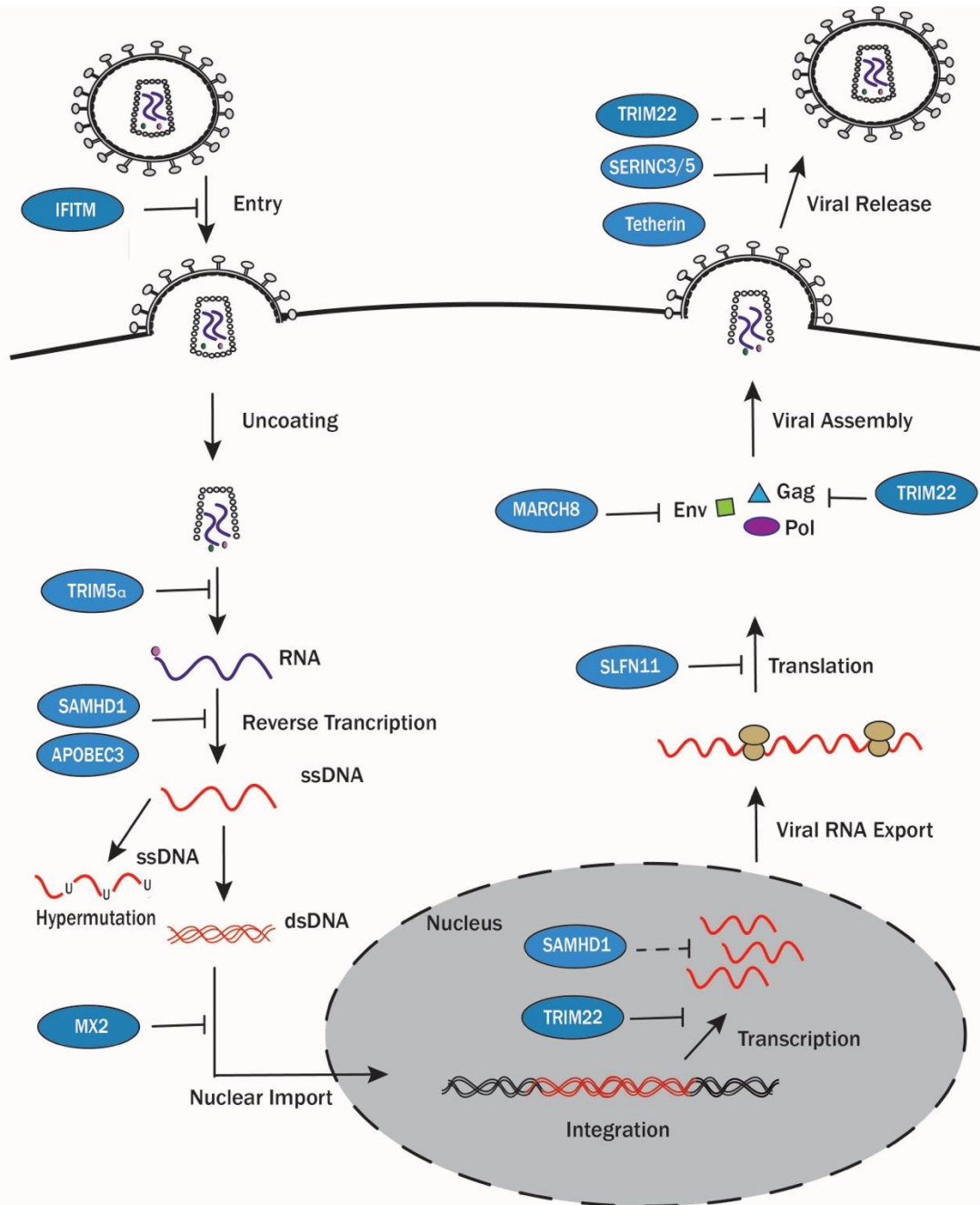


Figure 1.1. Inhibition of HIV replication by known host restriction factors

HIV-1 is inhibited by multiple restriction factors (blue) throughout its life cycle. IFITM proteins alter plasma membrane fluidity, inhibiting HIV-1 entry. TRIM5 α prevents appropriate uncoating

of the capsid. SAMHD1 inhibits cDNA synthesis by limiting the amount of free 2'-deoxynucleoside 5'-triphosphates (dNTPs) and possibly by its exonuclease activity (dashed lines). APOBEC3 proteins interfere with reverse transcription leading to uracilation of single-stranded DNA (ssDNA), a mechanism known as hypermutation. MX2 interferes with nuclear import, limiting the integration of proviral DNA. SLFN11 inhibits the translation of essential proteins needed to form HIV-1 virions. MARCH8 inhibits the incorporation of Env proteins. TRIM22 inhibits the production and incorporation of Gag proteins and inhibits LTR-dependent transcription. Tetherin, SERINC3/5, and TRIM22 prevent the virion from successfully budding. Dashed lines indicate proposed mechanisms. The pink circle denotes reverse transcriptase and the green circle denotes integrase, both packaged with the virion.

Restriction Factors	HIV-1 Evasion Mechanism
SAMHD1	Vpx inhibits SAMHD1 by recruiting an E3 ligase leading to its ubiquitylation and degradation
APOBEC3	Vif inhibits APOBEC by leading to its polyubiquitylation and proteosomal degradation
MX2	Capsid mutates to evade interaction with MX2 binding loop
SERINC3/5	Nef inhibits SERINC3/5 by decreasing its incorporation into virions and redistributing the proteins into an endocytic compartment
Tetherin	Vpu inhibits trafficking of tetherin to the surface and promotes its ubiquitylation and degradation

Table 1.1: Mechanisms of HIV-1 evasion

Restriction factors are listed with the major adaptive strategy that HIV-1 employs to evade their restriction.

CHAPTER II

Identification of CMPK2 and BCL-G as Interferon Stimulated Genes that Restrict HIV-1 Infection

El-Diwany, R., **Soliman, MG**, Sugawara, S. et al., CMPK2 and BCL-G are associated with type 1 interferon-induced HIV restriction in humans. *Sci Adv*, 2018. 4(8): p. eaat0843.

Abstract

Type 1 interferons upregulate hundreds of interferon-stimulated genes (ISGs) that have diverse antiviral effects. ISGs that restrict HIV-1 in humans have been poorly characterized. Exogenous interferon- α decreases HIV-1 viremia so we hypothesized that observed decline in HIV-1 viremia in people who receive exogenous interferon-alpha is due to the induction of ISGs that directly control HIV-1 in activated CD4+ T cells, the cells in which the virus chiefly replicates. To address this hypothesis, we previously published work characterizing putative ISGs that are HIV-1 restriction factors. Briefly, activated CD4+T-cells (CD3+/CD4+/CD38+/HLA-DR+) sorted from PBMCs taken from 19 HIV-1 infected patients with uncontrolled viremia before and after peginterferon alpha 2b (IFN) administration. RNAseq was performed on sorted activated CD4+ T cells and ISGs were identified in which Cytidine/Uridine Monophosphate Kinase 2 (CMPK-2) and Apoptosis facilitator Bcl-2-like protein 14 (BCL-G) were amongst the top hits that correlated in magnitude of induction with the subsequent decline in plasma HIV-1 viremia. *In vivo* findings were confirmed in both MT4 and THP-1 cells; cell lines in which BCL-G and CMPK2 are highly expressed upon IFN induction. mRNA (measured by qPCR) and protein levels (measured by Western blot) were quantified pre and post- IFN α treatment (1000 IU/mL). RNA interference was used to test whether the anti-HIV-1 effect of IFN α could be attributed to the gene of interest. IFN α -mediated restriction of HIV was attenuated in cells transfected with siRNA against CMPK2 in comparison to the scrambled control. The effect was approximately ten-fold with this effect seen across a range of HIV inocula. CMPK2, a gene involved in maintenance of intracellular UTP/CTP, is an ISG with potential to restrict HIV-1 replication. Overexpression was used to test the anti-viral effect of BCL-G on HIV-1 infection. The effect was minimal at

approximately three-fold inhibition observed in comparison to the empty control vector. It was hypothesized that BCL-G may be restricting HIV-1 replication through inducing apoptosis in infected cells. Analysis of RNaseq results shows multiple co-expressed genes Pre-IFN, Post-IFN, and Post-ART that may aid in facilitating BCL-G's restriction of HIV-1. Future work will focus on the mechanism underlying the antiviral effects of CMPK2 and BCL-G.

Introduction

HIV-1 infects 37 million people and contributes to approximately 1 million deaths per year. HIV-1 is controlled by lifelong treatment with combination antiretroviral therapy (cART), which acts by suppressing viral replication. IFNs upregulate transcription of diverse ISGs with numerous antiviral functions. Administration of exogenous IFN to HIV-1 infected individuals results in a decline of viral RNA levels and cells harboring HIV-1 by upregulation of these antiviral host defense mechanisms [128]. Because of their potential to uncover steps in the viral life cycle that are vulnerable to interruption, other interferon-induced HIV-1 restriction factors such as SAMHD1, BST2, and MX2 have become the focus of considerable research. Previous studies suggest that not all interferon-induced HIV-1 restriction factor have been characterized. Our lab characterized BCL-G and CMPK2 as interferon-induced HIV-1 restriction factor [129].

CMPK2 was first characterized as a pyrimidine nucleoside monophosphate kinase that localizes in the mitochondria, with a possible role in mitochondrial DNA depletion. CMPK2 was also shown to phosphorylate dUMP, dCMP, CMP, and UMP using ATP [130]. Intracellular levels of dUTP are detrimental to integration of HIV-1 proviruses. It was previously shown that in the presence of hUNG2 and high levels of dUTP, proviruses are highly uracilated, rapidly degraded,

and restricted from integrating [131]. We therefore hypothesized that CMPK2 may restrict HIV-1 infection by maintenance of intracellular UTP/CTP.

The role of BCL-G in the apoptotic pathway remains poorly understood. Initial studies of both the short and long isoforms of BCL-G demonstrated that BCL-G_S was capable of inducing apoptosis, while BCL-G_L weakly induced apoptosis [132]. The presence of the BH2 domain in the long isoform negatively regulates the ability to induce apoptosis. However, others have shown that the expression of the long isoform of BCL-G correlated with apoptosis of CD4⁺ T-cells in SLE patients [133]. We therefore hypothesized that BCL-G may restrict HIV-1 infection by causing apoptosis either directly or indirectly of infected CD4⁺ T-cells.

Materials and Methods

Human subjects. Nineteen individuals with HIV/HCV co-infection were recruited and enrolled in a study of HIV and HCV viral kinetics pre-antiretroviral therapy (pre-ART). These subjects were admitted to Johns Hopkins Hospital and a single shot of peginterferon alpha 2b (PEG-IFN) was administered. Blood was collected from these individuals at 24, 48, 72 hours, 7 days, and 14 days after IFN administration. The 19 individual's received cART consisting of raltegravir, tenofovir, and emtricitabine, 14 days post IFN. When individuals had taken cART for >12 weeks and showed evidence of HIV-1 suppression, a second PEG-IFN injection was administered. Blood was collected 72 hours later.

RNAseq and correlation between ISG upregulation and HIV-1 restriction. In the described cohort of 19 individuals, peripheral blood mononuclear cells (PBMCs) were collected Pre-IFN (0 hrs) and post-IFN (24 hrs) treatment and activated (CD38⁺HLADR⁺) CD4⁺ T cells were FACS

sorted at each respective time point. RNA was extracted, cDNA libraries were prepped, and RNA sequencing was performed (RNAseq). Putative ISGs were defined using RNAseq data. Fragments per kilobase million (FPKM) values were calculated Pre-IFN and Post-IFN, and induction of genes were calculated by dividing Post-IFN FPKM values by the Pre-IFN FPKM values. Putative ISGs that were HIV-1 restriction factors were defined by performing spearman rank-correlation, adjusted for multiple comparisons using Benajami-Hochberg method [134] between ISGs and the observed viral load decline within 24 hours of PEG-IFN treatment.

In Vitro HIV-1 Inhibition by IFN in multiple cell lines and measurement of HIV-1 production.

Nine cell lines MT4, THP-1, CXCR4-U87, CCR5-U87, pATC, PM1, supT1, MT2, and A3.03 (NIH AIDS Reagent Bank) were spinoculated with varying concentrations of HIV-IIIB (NIH AIDS Reagent Bank). For each concentration, 200,000 cells were spinoculated with HIV-IIIB and RPMI containing 10% FBS for 2 hours at 1,200g in V-bottom plates. Cells were rested overnight at 37 °C and each well was split into two wells; one received treatment with 1,000 IU/mL of universal Type I IFN (PBL), while the other received no treatment. All cells were incubated for 72 hours at 37 °C, and supernatants were collected for p24 measurements or TZM-bl assay to quantify luciferase activity. 10,000 TZM-bl luciferase reporter cells (NIH AIDS Reagent bank) were incubated with 100uL of supernatant and 100uL of DMEM containing 10% FBS and 20ug/mL of DEA-Dextran for 48 hours at 37 °C. Cells were washed two times with 1x PBS and lysed using 50uL of 1X cell culture lysis buffer (Promega). After incubation for 10 minutes, 50uL of lysed cells were transferred to a Costar 96 well white, flat-bottom plate for reading by the luminometer. Luciferase activity was measured using the Luciferase assay kit (Promega).

Infection was calculated by dividing the luciferase reading for the IFN-treated wells by the untreated wells.

Western Blots for measuring IFN induction, overexpression, and knockdown. MT4, THP-1, and 293T/17 (NIH AIDS Reagent Bank) cell lines were used for western blot experiments. 750,000 cells were plated in 6-well plates for 24 to 72hrs with varying concentrations of universal Type I IFN (0,100, and 1,000 IU/mL). Cells were lysed using 1x cell lysis buffer with protease inhibitors (1:100; Cell signal) on ice for 20 minutes. Cell lysates were collected after centrifugation at 4°C, for 20 minutes, at 13,000g. Protein was quantified using the BCA assay (Thermo) and 10ug of lysate was loaded into each well of 4012% bis-tris gels (NuPage). Blots were incubated for 1 hour at room temperature in 5% MILK in 1x TBS + 0.1% Tween-20. Primary antibody for CMPK2 (1:500, Novus), MX2 (1:1000, Novus), BCL-G (1:500, Novus), Anti-HA (1:1000, Thermo), and Actin (1:10,000, Thermo) was incubated overnight at 4°C in 5% MILK in 1x TBS + 0.1% Tween-20.

In vitro knockdown experiments and measuring HIV-1 production. MT4 or THP-1 cells were transfected using electroporation with SMARTpool siGENOME siRNAs (Dharmacon) against our gene of interest or with scrambled negative controls at 100nM. Electroporation was done according to the manufacturer's protocol using Amaxa Cell Line Nucleofector Kit V (Lonza). Immediately after electroporation, cells were rested in recovery media overnight at 37°C. 200,000 cells were spinoculated with varying concentrations of HIV-IIIB in 50uL of RPMI containing 10% FBS for 2 hours at 1,200g in V-bottom plates. Cells were rested overnight at 37°C and each well was split into two wells; one received treatment with 1,000 IU/mL of

universal Type I IFN (PBL), while the other received no treatment. All cells were incubated for 48 hours at 37 °C, and supernatants were collected for the TZM-bl assay as described above.

Overexpression of BCL-G, co-expression with HA-BCLXL and DN-Caspase9. pCMV-Myc-BCL-G was previously cloned [129] and used alongside the empty pCMV-Myc_N (Clontech) vector as a control. 293T/17, COS-7, CXCR4-U87, and CCR5-U87 cell lines were plated at 750,000 cells per well in a 6-well plate. 24 hours later, the pCMV-Myc-BCL-G and empty control vector were transfected with lipofectamine 2000 according to the manufacturer's protocol. Briefly, 2ug of each plasmid was transfected with 10uL of lipofectamine 2000 (Thermo) and incubated for 24, 48, or 72 hours at 37 °C. HA-BCLXL and DN-Caspase 9 plasmids were gifted courtesy of Dr. Marie Hardwick at the Johns Hopkins School of Public Health. Co-expression experiments with pCMV-Myc-BCL-G was done using various amount of HA-BCLXL or DN-Caspase9 plasmids DNA (0ug-2ug) and transfected using Lipofectamine 2000 as described above. Cells were lysed for Western blot analysis as described above.

Overexpression of BCL-G and the effect of MG132. 293T/17 cell line was plated at 750,000 cells per well in a 6-well plate. 24 hours later, the pCMV-Myc-BCL-G vector was transfected with lipofectamine 2000 according to the manufacturer's protocol, and incubated for 48 hours at 37 °C. At 48 hours cells were either treated with 20uM of MG132 (Sigma) or left untreated for 4, 8, 12, 24, or 48. After incubation, cells were lysed for western blot analysis as described above.

Overexpression of BCL-G and quantitative real time PCR (qPCR) analysis of HIV-1 production.

HIV production assays were performed by plating 10,000 cells of 293T/17, COS-7, CXCR4-U87, or CCR5-U87 cell lines in 96-well flat bottom plates and incubated overnight at 37 °C. Cells were

transfected using 0.5ug of pCMV-Myc-BCL-G or pCMV-Myc_N with 0.5uL of lipofectamine 2000 per well. 48 hours later cells were infected with HIV-IIIB at varying concentrations in 100uL of DMEM and 10% FBS. 24 hours later supernatants were collected and 100uL were placed on TZM-bl cells for the HIV production assay. The cells were lysed using the ZR-Duet DNA/RNA Miniprep lysis buffer (Zymo Research). Reverse transcription was performed using Multiscribe reverse transcriptase kit (Thermo) according to the manufacture's protocol. First minus strand transfer cDNA products and Poly adenylated tail were detected using the primer/probe combination as previously described, and samples were normalized to geometric means of the CT values from the housekeeping genes, GAPDH and RPLP0. Integrated HIV-1 DNA was quantified using Alu PCR as previously described [135]. Values were normalized to geometric means of the CT value for ERV3. qPCR reactions were performed in duplicates using the PrimeTime Gene Expression Master Mix (IDT).

Statistical Analyses using R studio. All correlations were performed using the package "psych" in R version 3.6.1, using spearman rank correlations method. To identify the top genes that were co-expressed with BCL-G Pre-IFN, Post-IFN, or post-ART treatment, statistically significant spearman rank coefficients ($p < 0.05$) were calculated between BCL-G and the observed genes. The post-ART timepoint FPKM values were obtained 72 hours post the second treatment with IFN as described above. Correlations were also performed to assess putative restriction factors between the fold-changes of putative ISGs and the intercellular associated HIV-1 DNA. Pairwise correlations were performed using the "corrplot" version 0.84. K-means clustering and principle component analysis were performed using the "PerformanceAnalytics" package.

Results

HIV-1 restriction by IFN. In order to test the hypothesis that CMPK2 and BCL-G are ISGs that restrict HIV-1 infection from our previous work [129], we needed to test for robust IFN-mediated restriction of HIV-1 replication in cell lines. We assayed nine cell lines by infecting them with a titrated range of replication-competent HIV-1 strain. Half of the wells for all cell lines were treated with IFN to test for inhibition of viral replication. MT4 and THP-1 cells supported the replication of HIV-1 lab strains, while being the most susceptible to IFN-mediated inhibition (**Supplementary Figure 2.1**).

IFN inducibility of CMPK2 and the capacity to inhibit HIV-1 replication. We previously published data showing that CMPK2 mRNA was potently induced in THP-1 cells upon treatment with IFN [129]. We therefore studied CMPK2's restriction capabilities in THP-1 cells. We confirmed CMPK2 induction at the protein level in THP-1 cells. MX2 was used as a positive control of IFN-inducibility due to its identification as an ISG that restricts HIV-1 [70-72]. Both CMPK2 and MX2 were best induced at 48 hours post treatment with IFN (**Figure 2.1A**). To determine if IFN-mediated HIV-1 restriction could be attributed to CMPK2, we used siRNA to knockdown CMPK2 expression in THP-1 cells. We transfected THP-1 cells with pooled siRNA against CMPK2 or with scrambled controls. THP-1 cells with our scrambled siRNA resulted in restriction of HIV-1 by IFN. This IFN-induced restriction of HIV-1 was attenuated in THP-1 cells transfected with siRNA against CMPK2. This effect was 10-fold and observed over a range of HIV-1 inoculum (**Figure 2.1B**). HIV-1 titers in the untreated THP-1 cells were greater in the cells transfected with scrambled siRNA than in cells transfected with siRNA against CMPK2, supporting the role of CMPK2 as a restriction factor (**Supplementary Figure 2.1**). We further verified our results using western blots of the siRNA transfected THP-1 cells after knockdown and treatment with IFN to

ensure there was no upregulation of CMPK2. Our westerns showed no induction of CMPK2 after treatment with IFN (**Figure 2.1C**). However, CMPK2 was upregulated in THP-1 cells that were transfected with scrambled siRNA and left untreated with IFN. This was most likely due to innate signaling responses in THP-1 due to transfection of siRNA.

Mechanism of HIV-1 restriction by BCL-G.

We previously demonstrated that overexpression of BCL-G using a myc-tag system resulted in restriction of HIV-1 replication in MT4 cells [129]. To develop a model in which we could test for restriction of replication-competent HIV strains, we tested CXCR4-U87 and CCR5-U87 cell lines that support replication of X4 and R5 tropic viruses, respectively. Myc-tagged BCL-G was overexpressed in CCR5-U87 cells (**Supplementary Figure 2.2**). CCR5-U87 cells were transfected with myc-tagged BCL-G for 48 hours, followed by a 24-hour infection with a range of HIV-IIIB inoculum and restriction of HIV-1 was measured using the TZM-bl assay. Our results showed minimal restriction of HIV-1 replication in comparison to the empty-myc control, with the greatest restriction of half a log (**Figure 2.2A**). ISGs act by restricting HIV-1 during various stages of its life cycle. It was previously reported that IFN treatment blocked the accumulation of all HIV cDNAs [136]. To assess if BCL-G restricts HIV-1 during reverse transcription of viral products, we ran qPCR to test for levels of first (minus) strand cDNA. CCR5-U87 cells were transfected with myc-tagged BCL-G, myc-tagged MX2 as a positive control, and the empty Myc-tagged vector. Cells were infected with HIV-IIIB across two-fold dilutions of inoculum. Western blots images show similar degradation pattern as reported earlier (**Supplementary Figure 2.3**). Our results showed no significant accumulation in first stand cDNA products, indicating that BCL-G was not inhibiting HIV-1 during reverse transcription (**Figure 2.2B**). To measure the

amounts of HIV-1 virions in our assays, we ran qPCR quantifying HIV-1 RNA as described before [137]. Our results showed no significant difference in HIV-1 RNA across all conditions (**Figure 2.2C**).

The role of BCL-G in Apoptosis during HIV-1 Infection

In our previous published work, we were unable to visualize BCL-G in MT4 cells upon treatment with IFN. In order to find antibodies most sensitive to detecting the BCL-G, we transfected the myc-tagged BCL-G vector into 293T/17 cells. Our results were visualized using western blots, in which we noticed a ladder pattern in wells with our BCL-G vector 48 and 96 hours post transfection (**Figure 2.3A**). This pattern has been previously described as protein degradation [138]. In attempts to reverse degradation of BCL-G, we treated 293T/17 cells with MG132, a commonly used proteasome inhibitor. MG132 had minimal effect on degradation of BCL-G, demonstrating that BCL-G was being degraded through a different pathway (**Figure 2.3B**). BCL-G has previously been described to have both pro-apoptotic [133] and anti-apoptotic capabilities [139]. We therefore hypothesized that another mechanism BCL-G may restrict HIV-1 infection is through the induction of apoptosis in infected cells. We obtained a HA tagged BCL-XL vector from Dr. Marie Hardwick to test this hypothesis. BCL-XL has been described in literature to inhibit apoptosis by sequestering pro-apoptotic proteins [140]. To address the controversial literature describing BCL-G, we co-transfected the myc-tagged BCL-G vector with equivalent amounts of the HA-BCL-XL vector and visualized protein expression by western blot. Our results showed that BCL-G expression was increased in the presence of BCL-XL, providing a system in which BCL-G levels can be modulated (**Figure 2.3C**). Our data suggests that BCL-XL regulates BCL-G levels by either sequestering BCL-G or modulating BCL-G levels to either

enhance or diminish its downstream role. Further studies need to be done to understand this relationship in greater detail.

Determining genes that relate to expression of BCL-G Pre-IFN, Post-IFN, and Post-ART.

With the unclear role of BCL-G in initiating apoptosis in HIV-1 infected cells, we hypothesized that BCL-G's expression might be dependent on other genes involved in the apoptosis pathway, during the Pre-IFN, Post-IFN, or Post-ART timepoints. To analyze genes that related to BCL-G Pre-IFN, we took FPKM values of all genes from the RNAseq dataset and correlated it BCL-G expression among all 19 individuals, and plotted the top ten significant genes (**Figure 2.4A**). Spearman rank coefficients were calculated and the top fifty statistically significant genes were analyzed (**Figure 1.4B**). Pairwise correlation analysis revealed clusters of related genes, and as expected, the top fifty genes were highly related within each other, with Spearman coefficients >0.6 or >-0.6 . (**Figure 2.4C**). We further characterized clustering using the principal component analysis of FPKM values. There was distinct clustering of genes that negatively or positively correlated with BCL-G expression, as well as clusters of previously defined ISGs (**Figure 2.4D**). Interestingly, BCL-G was highly correlated with CMPK2, MX2, and LAMP3 Pre-IFN, which were all described as ISGs in previously published work. It was most highly correlated with LAP3, a cytosolic aminopeptidase, with a proposed role in apoptosis [141]. A heatmap analysis was performed with a clustering filter to demonstrate the highly related group of ISGs, seen in the PCA analysis (**Supplementary Figure 2.4**). This analysis was performed for the Post-IFN timepoint by correlating the fold change of BCL-G with the fold change of all genes in our RNAseq data. Fold change was calculated by dividing the FPKM values Post-IFN by the FPKM values Pre-IFN. Pair-wise correlation analysis revealed clusters of related genes (**Figure 2.4E**).

Finally, the analysis was performed for the Post-ART timepoint, revealing another unique cluster of related genes (**Figure 2.4F**). This analysis demonstrated consistencies in relatedness of BCL-G with previously defined ISGs or members of the interferon response pathways, at all timepoints (i.e. IFI44, IFI6, IRF7, and MX2). It also revealed relatedness of BCL-G with other possible players in the apoptosis pathway at all timepoints (ie. LAP3 and tumor necrosis factor ligand superfamily member [TNFSF] proteins). The analysis suggests that BCL-G might be regulated alongside other genes that induce apoptosis or restriction in HIV-1. Further analysis will parse out the relatedness of these genes with BCL-G *in vitro*.

Discussion and Limitations

We were the first to annotate both CMPK2 and BCL-G as ISGs that restrict HIV-1 infection. CMPK2 has previously been described as an ISG, however its antiviral effect has been minimally explored. We aimed to explore the mechanism in which CMPK2 restricts HIV-1 infection. Because its enzymatic activity is directed towards phosphorylating dUMPs to dUTPs [130], we hypothesized that a possible mechanism for inhibiting HIV-1 infection was through increasing intracellular stores of dUTP. It was previously published that high pools of dUTP causes uracilation in HIV-1 proviruses, inhibiting its integration [131]. This mechanism would be a novel method in which an ISG restricts HIV-1 infection. Most importantly, inhibition pre-integration is critical, as the establishment of a latent reservoir is one of the largest hurdles to curing HIV-1. We faced many challenges when further studying the mechanism of restriction by CMPK2. The baseline induction of CMPK2 using siRNA was limiting our full study of its mechanism, so we developed a knockout cell line using CRISPR/Cas9 technology in THP-1 cell lines. Through the process of development, THP-1 cells died during the process of enriching clonal populations of

cells with knocked out CMPK2, likely due to toxicity from puromycin. The remaining cells began to differentiate into macrophages, a process that can classically be initiated using PMA in THP-1 cells, most likely due to cellular stress.

BCL-G was also previously described as an ISG without a known antiviral effect. Once we demonstrated its restriction of HIV-1 infection, we aimed to study the mechanism in which it restricts HIV-1 infection. BCL-G has a controversial role in the literature with some studies showing it is pro-apoptotic [132-133], while other studies show it is anti-apoptotic [139]. We hypothesized one mechanism in which BCL-G restricts HIV-1 is by inhibiting HIV-1 at various stages of its lifecycle, early in infection. Our data shows that BCL-G does not directly inhibit HIV-1 during first strand synthesis or by directly targeting HIV-1 RNA levels. We also tested for the accumulation of 2-LTR circles and integrated HIV-1 DNA, but our qPCR assays were insufficient at detecting both in infected CCR5-U87 cells. We then hypothesized another mechanism BCL-G restricts HIV-1 infection is through causing apoptosis of infected cells. When we first transfected BCL-G into 293T/17 cells and visualized our results using western blots, we noticed the laddering pattern of the protein, an indication of protein degradation. Our data suggests that BCL-G is not being degraded through the proteasome, and therefore another mechanism is causing its degradation. In collaboration with Dr. Marie Hardwick, we obtained tools to study the role of BCL-G in the apoptotic pathway. Previously, studies have shown that one mechanism pro-apoptotic genes are inhibited is through sequestration of pro-apoptotic genes by anti-apoptotic genes like BCL-XL. We tested the hypothesis that BCL-XL plays a role in regulating BCL-G in CCR5-U87 cells. Our results showed that BCL-XL increases expression of BCL-G and its degradation products. Further work needs to be done in order to answer whether

BCL-XL is binding BCL-G itself, or signaling other players to induce expression. These results differ from previously published work in which co-transfection of BCL-G with BCL-XL shows no change in BCLG's overall protein expression [132]. Whether BCL-G induces apoptosis remains inconclusive in the context of HIV-1 infection, due to limitations in our assay development. We experienced difficulty in developing an assay in which sufficient HIV-1 replication was quantified, and transfection with the transfection reagent alone, didn't induce restriction of HIV-1. We assayed five different cell lines, with CCR5-U87 being the most promising cell line. Cells were counted from the HIV-1 restriction experiment above (**Figure 3A**) and cell counts were similar across all conditions (data not shown).

The hypothesis that BCL-G may play a role in apoptosis is feasible given it has previously been shown to be enhanced in expression in pathogenic SIV infection in rhesus macaques, but not in nonpathogenic SIV infection in African green monkeys [142]. One notable difference between the pathogenic and nonpathogenic SIV strains is the loss of CD4+ T-cells in the pathogenic strain, similar to natural HIV-1 infection in humans. Many of the BCL-2 family members have been previously described to skew infected CD4+ T cells towards a pro- or anti-apoptotic fate. However, HIV-1 viral proteins have also developed mechanisms to inhibit various pro-apoptotic proteins. For example, the protein Nef has been shown to phosphorylate and inactivate the protein BAD, as well as downmodulate the expression of p53, inhibiting apoptosis [143]. BCL-G has been shown to have p53 binding sites, posing a mechanism in which BCL-G can indirectly inhibit HIV-1 infection [144]. Overall our results provide evidence that CMPK2 and BCL-G are ISGs that restrict HIV-1 infection, providing novel potential small molecule inhibitors as therapeutics for HIV-1 infection control.

Figures

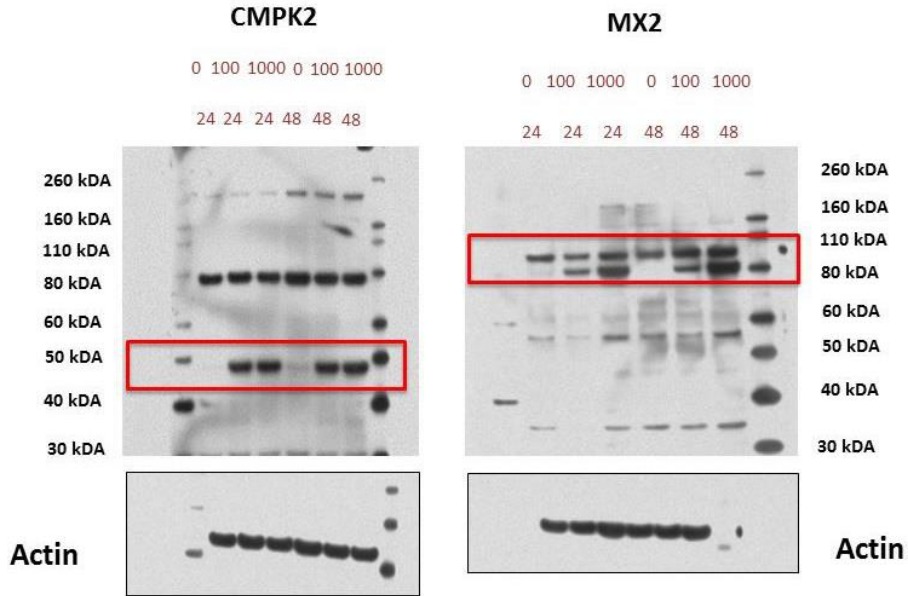


Figure 2.1A: CMPK2 and MX2 proteins are induced by IFN in THP-1 and MT4 cells. Western blots showing the upregulation of CMPK2 and MX2 after treatment with 1000 IU/mL of IFN for 24 and 48 hours. CMPK2 and MX2 induction.

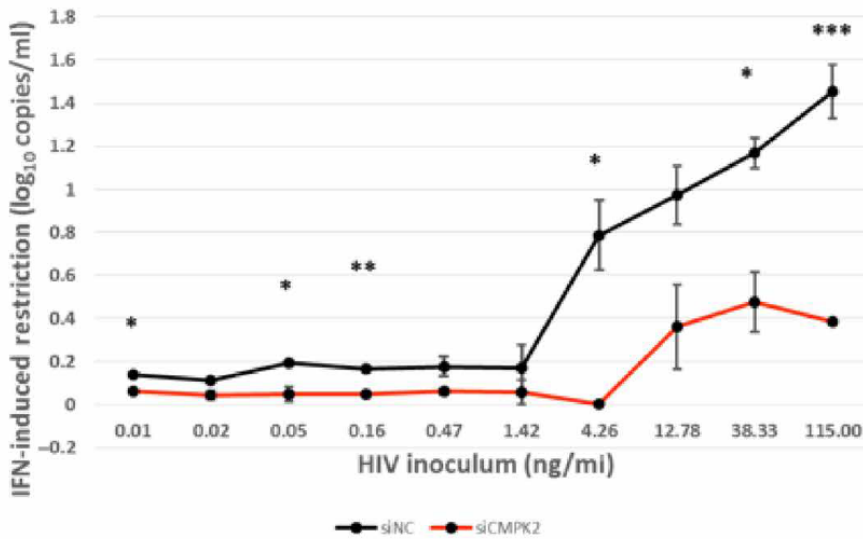


Figure 2.1B: Restriction of HIV in vitro is dependent on the IFN induction of CMPK2.

Knockdown of CMPK2 was performed using pooled siRNA against CMPK2 in THP-1 cells (red) and was compared to the scrambled control (black). Cells were inoculated with varying concentrations of HIV-IIIB (115ng/mL-0ng/mL) and split to be treated with IFN or left untreated. Replication was quantified using the TZM-bl luciferase assay. IFN-induced restriction was calculated by log-transforming the difference in RLU values between the IFN-treated and untreated cells across each condition. *P,0.05; **P<0.01;***P<0.005.

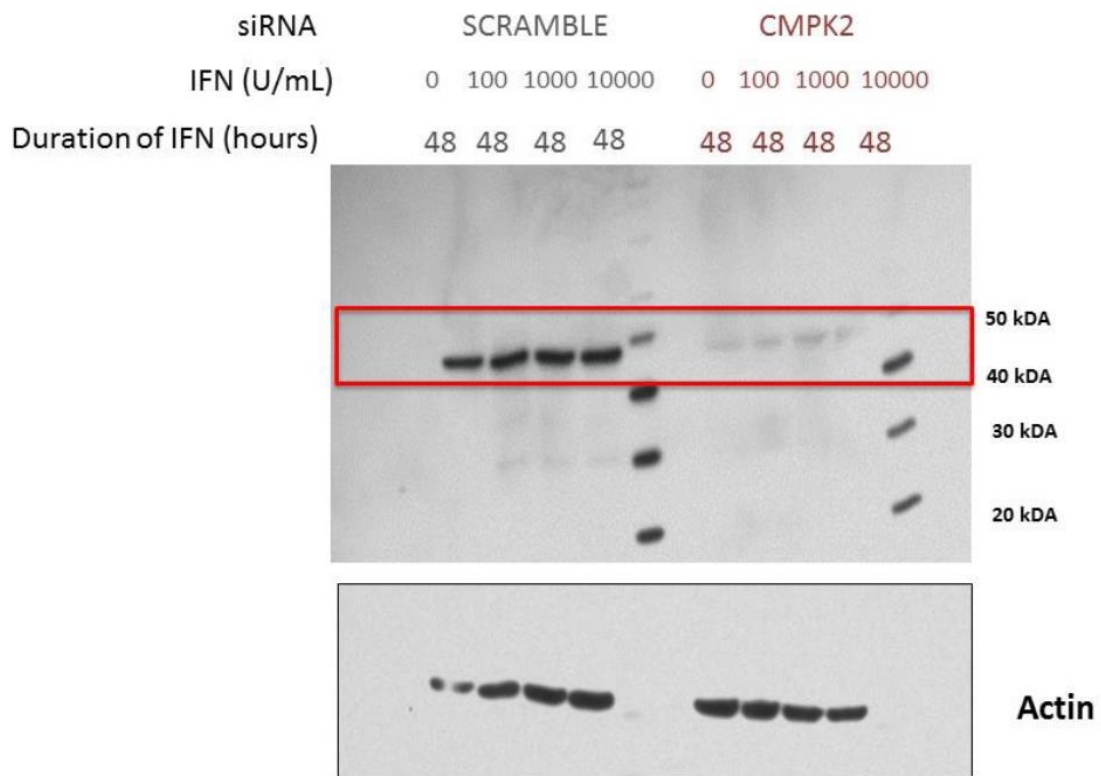


Figure 2.1C: CMPK2 knockdown using siRNA in THP-1 cells. Western blots showing the knockdown of siRNA in THP-1 cells. To ensure knockdown, THP-1 cells were treated with IFN at varying doses for 48 hours.

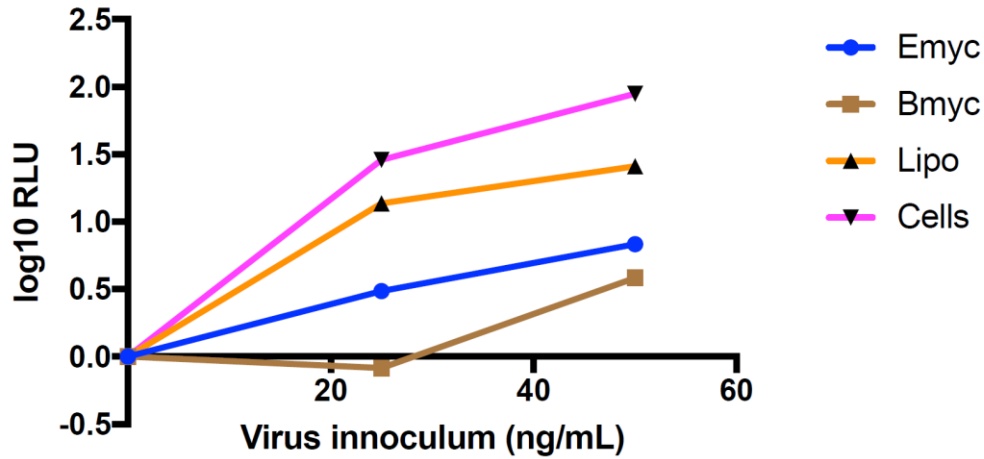


Figure 2.2A: Overexpression of BCL-G minimally inhibits HIV infection on CCR5-U87 cell. Cells were transfected with myc-tagged BCL-G (brown), the empty myc-vector (blue), transfection reagent (orange), or untransfected (pink) into CCR5-U87 cells. After 48 hours of transfection, cells were infected with 50, 25, or 0 ng of HIV-IIIB. Infection was measured using the TZM-bl assay. RLU values were log-transformed to indicate the level of HIV restriction (y-axis) across varying concentrations of HIV inoculum (x-axis). Each condition was tested in duplicate and the geometric means are shown above.

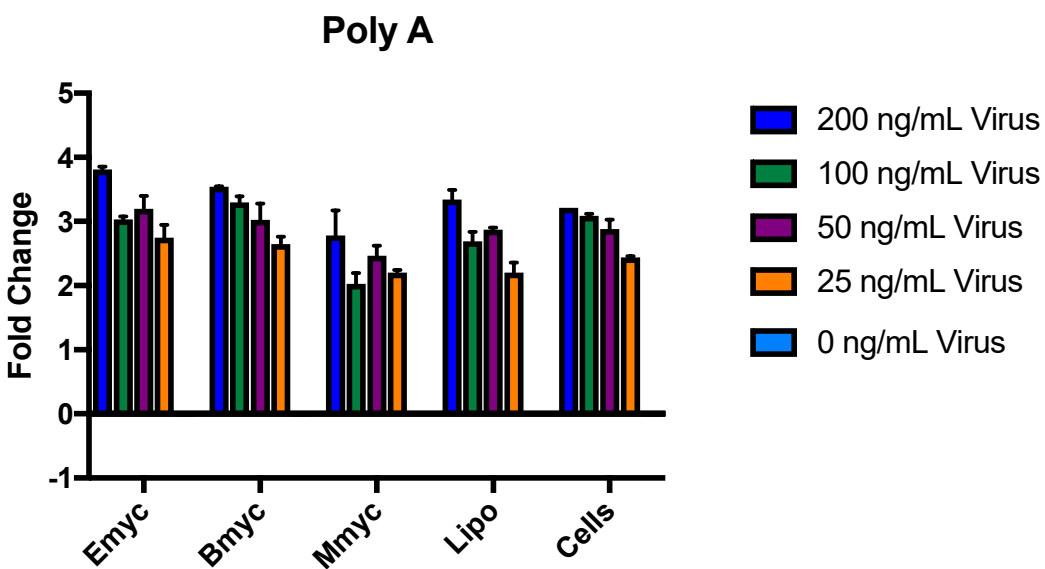


Figure 2.2B: Overexpression of BCL-G-myc does not inhibit HIV RNA. CCR5-U87 cells were transfected with myc-tagged BCL-G, myc-tagged MX2, empty myc vector, transfection reagent alone (Lipo), or untransfected (cells) for 48 hours and infected with HIV-IIIB at varying inoculum. qPCR data showing the fold change of production of HIV-1 RNA in each condition, relative to housekeeping genes. All samples were run in triplicate and there were no statistically significant differences between the conditions.

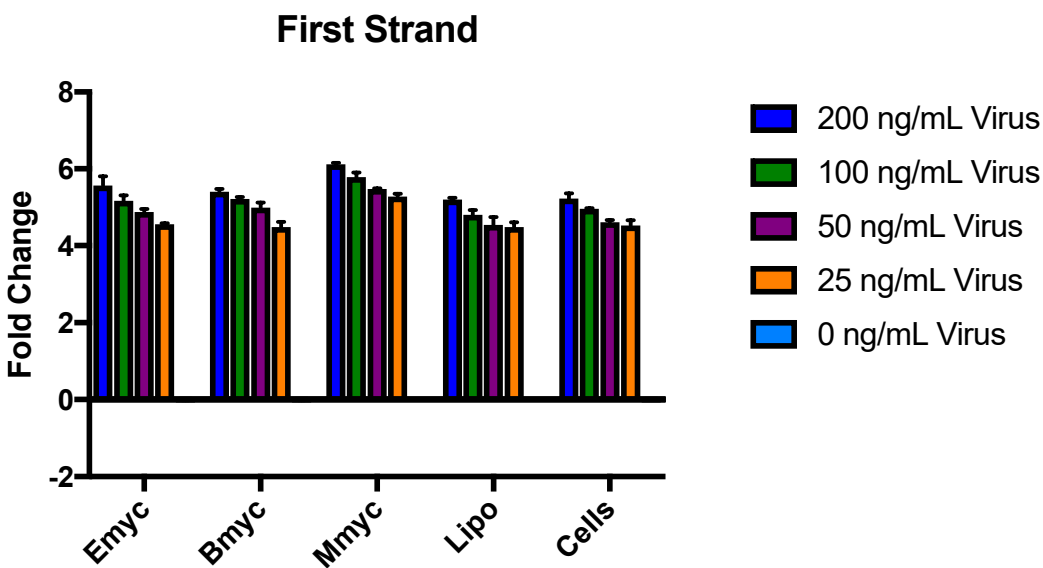


Figure 2.2C: Overexpression of BCL-G-myc does not inhibit production of first (minus) strand cDNA. CCR5-U87 cells were transfected with myc-tagged BCL-G, myc-tagged MX2, empty myc-vector, transfection reagent alone (Lipo), or untransfected (cells) for 48 hours and infected with HIV-IIIB at varying inoculum. qPCR data showing the fold change of production of HIV-1 RNA in each condition, relative to housekeeping genes. All samples were run in triplicate and there were no statistically significant differences between the conditions.

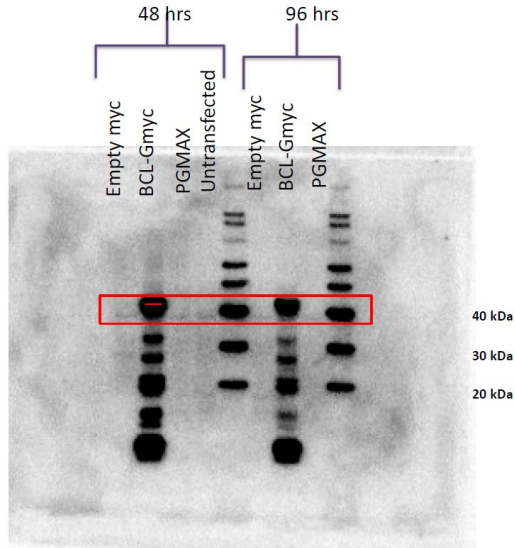


Figure 2.3A: BCL-G overexpression in 293T/17 cells causes degradation of BCL-G. 293T/17 cells were transfected with myc-tagged BCL-G, empty myc-tagged vector, pgMAX vector, or left untransfected. Western blots showing overexpression of BCL-G led to a degradation pattern at the protein level.

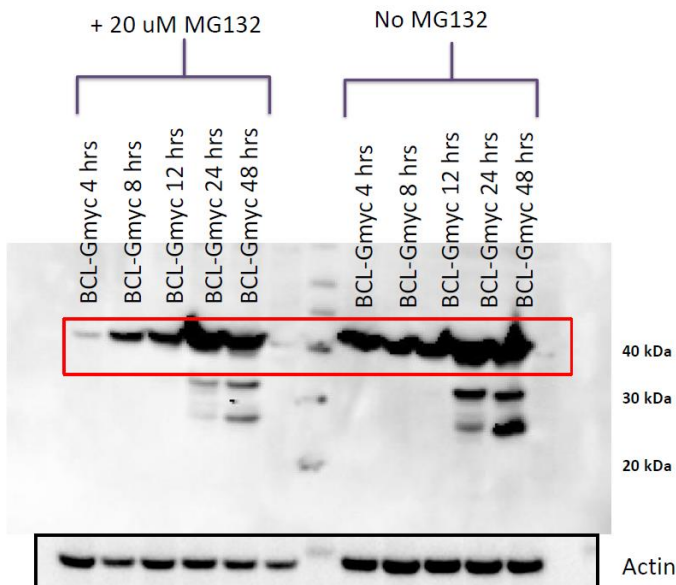


Figure 2.3B: MG132 treatment minimally rescues the degradation of BCL-G. 293T/17 cells were transfected with myc-tagged BCL-G and treated with MG132 at 4, 8, 12, 24, or 48 hours post-transfection. Western blots showing the degradation of BCL-G is minimally rescued by MG132.

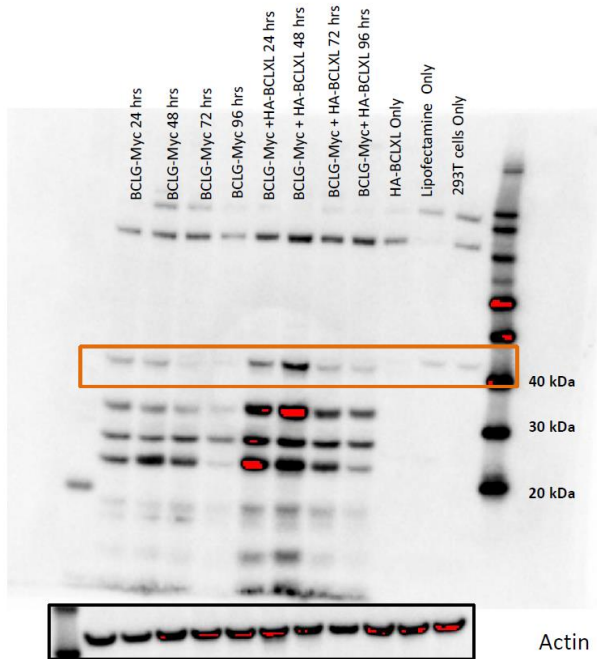


Figure 2.3C: Co-expression of BCL-G with BCL-XL causes an increase in protein levels of BCL-G and its degradation products. 293T/17 cells were transfected with myc-tagged BCL-G, HA-BCL-XL, transfection reagent alone (Lipofectamine) or left untransfected for 24, 48, 72, or 96 hours. Western blots showing the protein expression of BCL-G and its degradation products are increased when co-expressed with BCL-XL.



Figure 2.4A: Correlation plots of the top ten statistically significant genes. FPKM values of BCL-2 Pre-IFN were correlated with all FPKM values of our RNAseq dataset. The top ten statistically significant correlated genes are plotted above after analysis of spearman rank correlation coefficients. The genes are Lap3, DTYMK, MYD88, ZNF74P, RRP1, NUP50, SERPING1, IRF7, and FAF2. All r values are >0.6 and p-values are <0.005 .

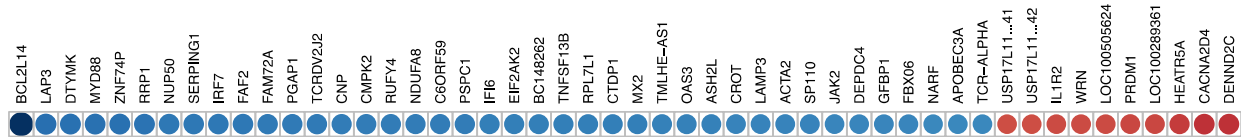


Figure 2.4B: The top 50 correlated gene with BCL-G Pre-IFN. The top fifty statistically significant genes are plotted above. The blue circles indicate a positive correlation coefficient, and the red circles indicate a negative correlation coefficient.

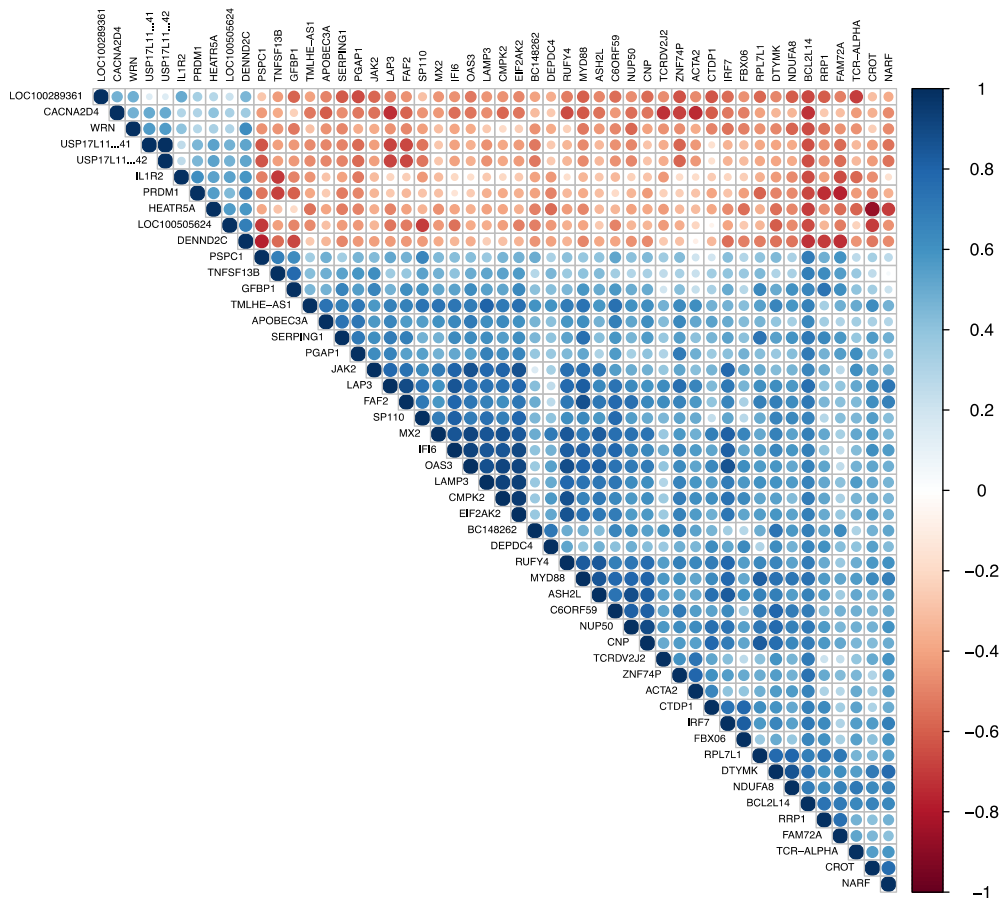
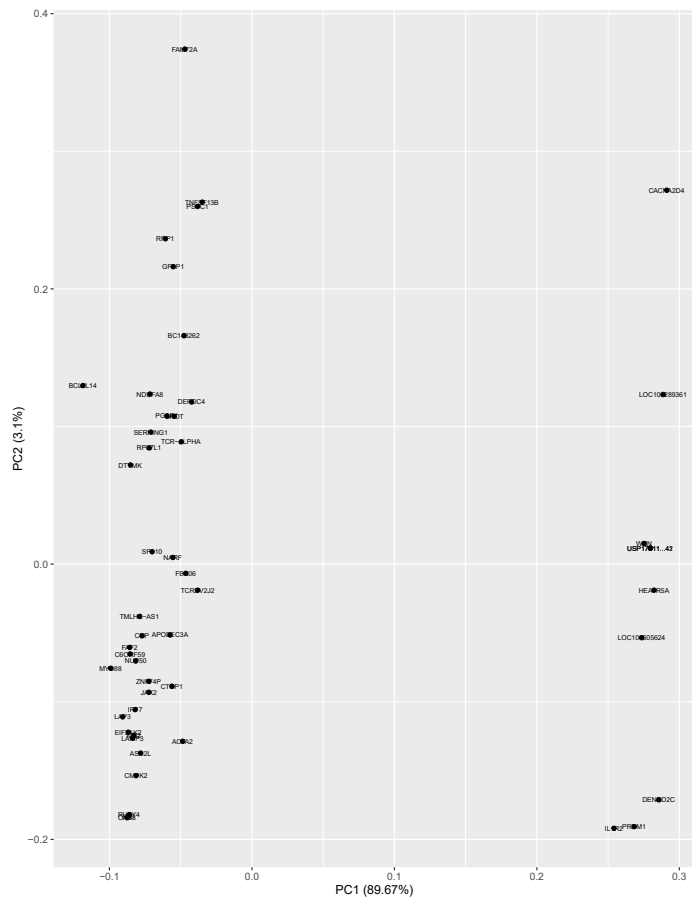


Figure 2.4C: Pairwise Correlation Plots for the top correlated genes Pre-IFN. Pairwise correlation plot of the top fifty genes revealed a hierarchy or relatedness among previously defined ISGs and among each other.



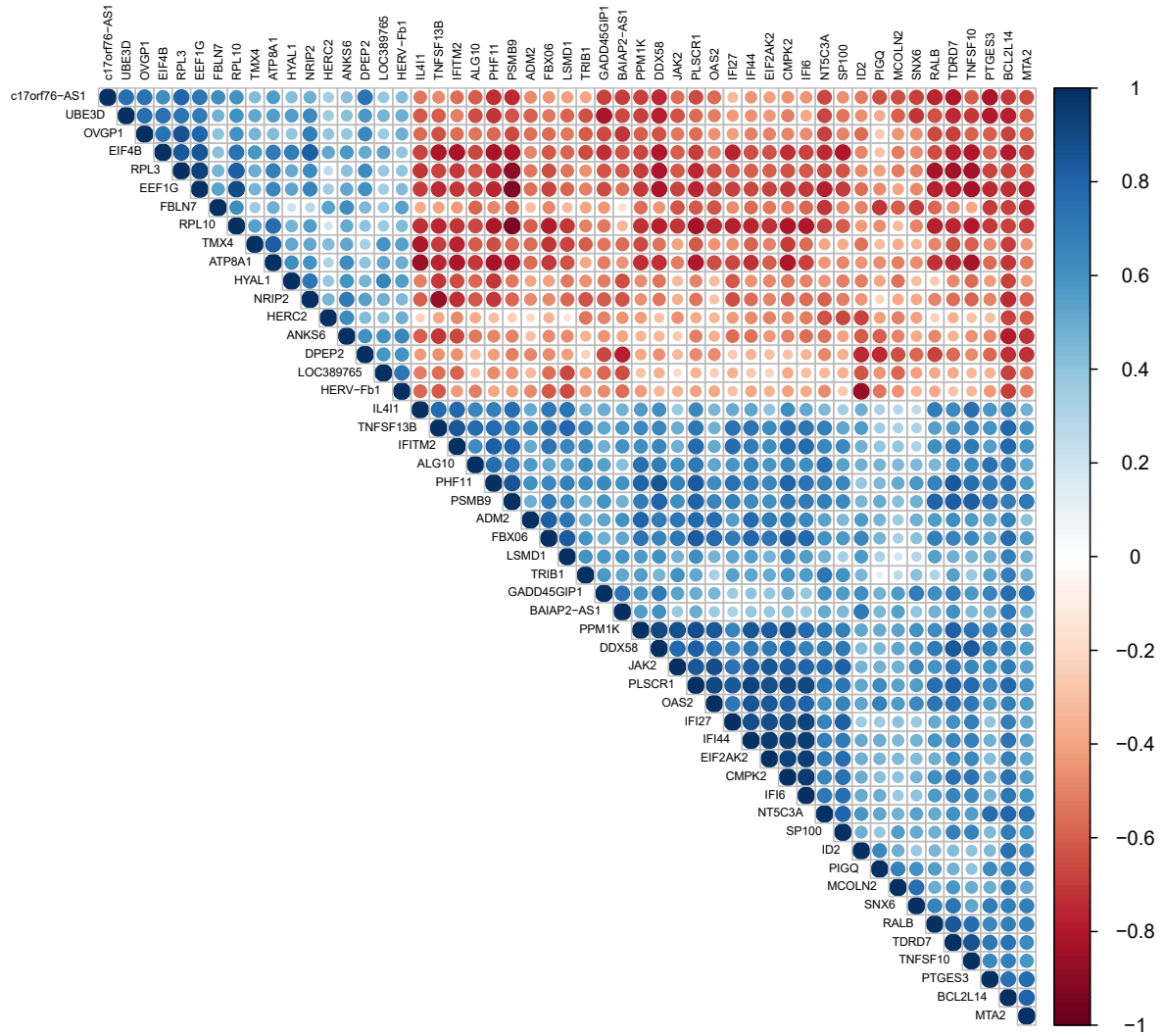


Figure 2.4E: Pairwise Correlation Plots for the top correlated genes Post-IFN. Pairwise correlation plot of the top fifty genes revealed a hierarchy or relatedness among previously defined ISGs and among each other.

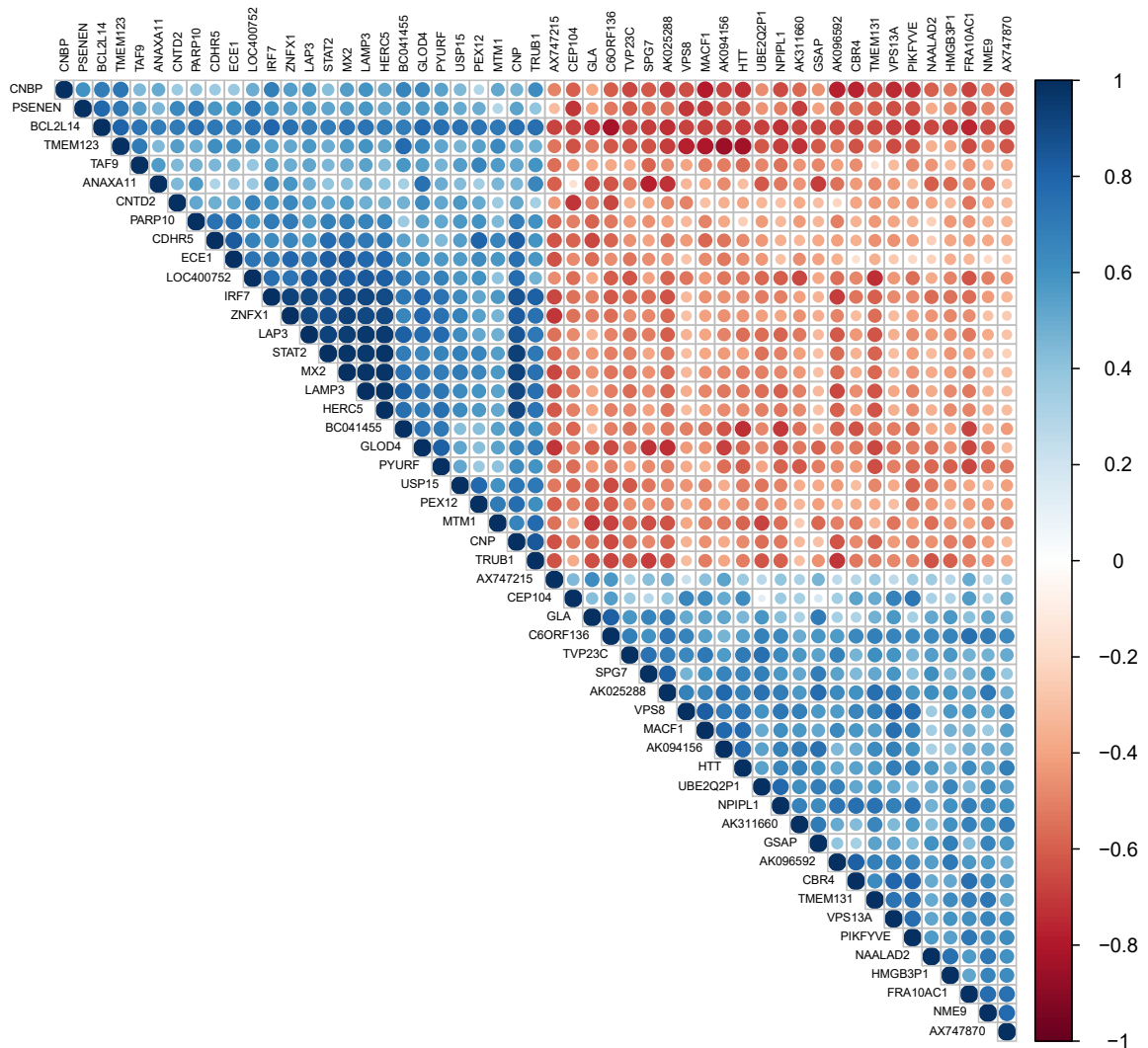
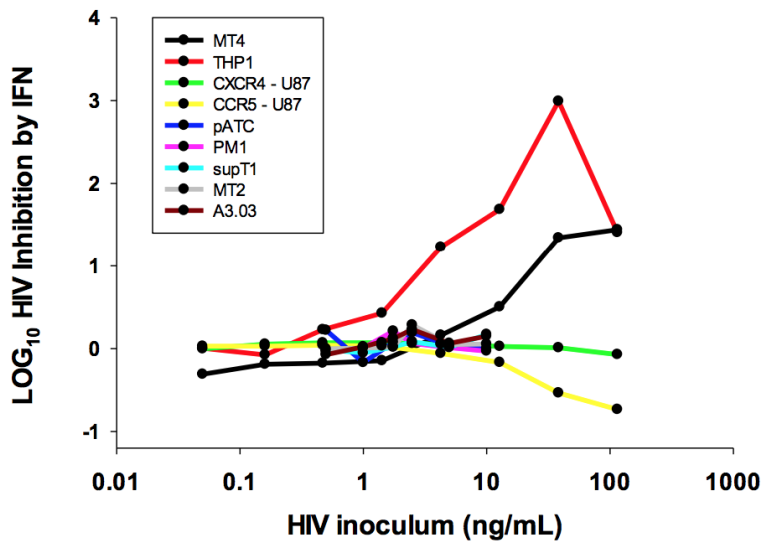
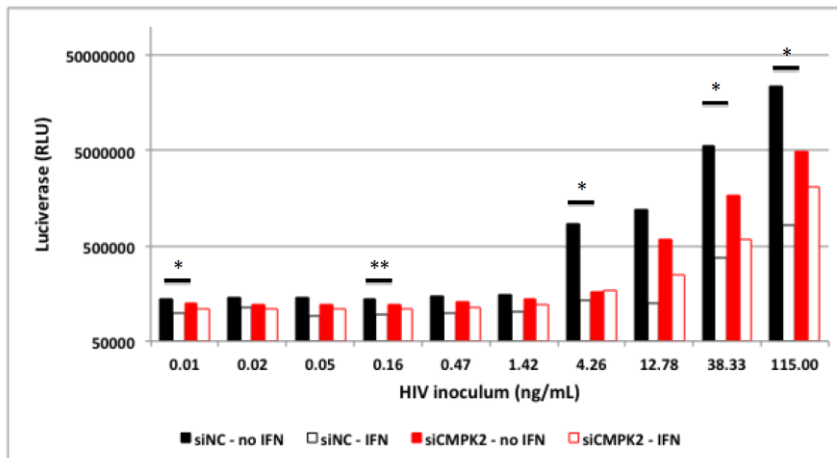


Figure 2.4F: Pairwise Correlation Plots for the top correlated genes Post-ART. Pairwise correlation plot of the top fifty genes revealed a hierarchy or relatedness among previously defined ISGs and among each other.

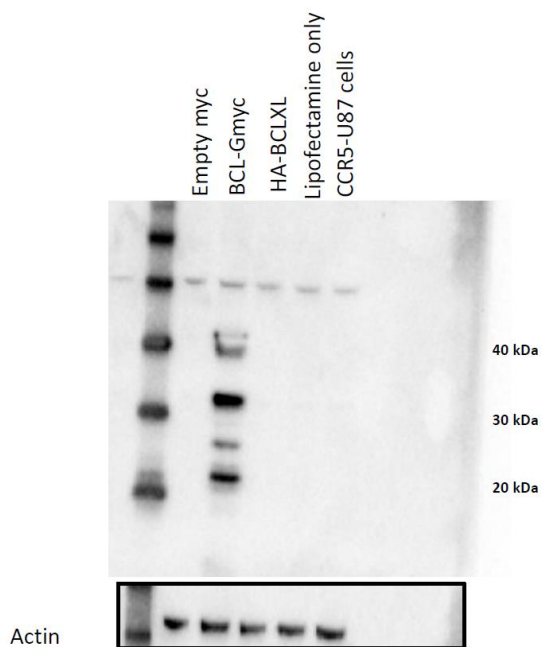
Supplementary Figures



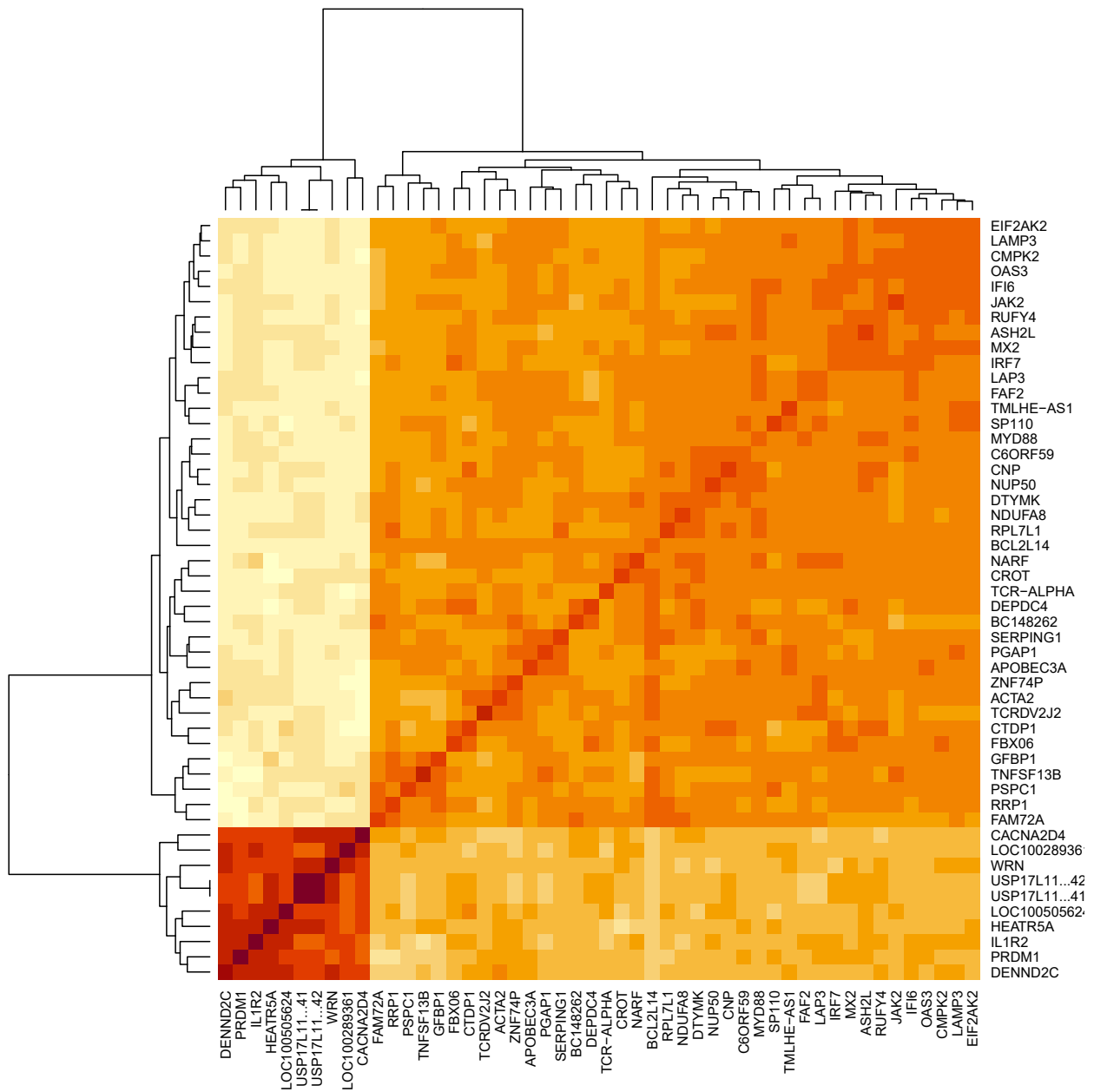
Supplementary Figure 2.1: IFN-mediated restriction of HIV-1 in various cell lines. Cell lines were infected with varying concentrations of HIV-IIIB for 24 hours. Cells were then left untreated or treated with 1000 IU/mL of IFN for 72 hours. HIV replication was measured using supernatants for the p24 assay or the TZM-bl assay. Inhibitions was calculated by subtracting the \log_{10} values of p24 or RLU values in IFN-treated cells from the untreated cells. The geometric means are plotted above.



Supplementary Figure 2.2: IFN restriction of HIV-1 in THP-1 cells is dependent on CMPK2. THP-1 cells were transfected with pooled siRNA against CMPK2 (red) or scrambled control (black). Cells were infected with varying concentrations of HIV-1 inoculum, and then split to either be treated with IFN (dashed) or left untreated (solid). Replication of HIV-1 was quantified using the TZM-bl assay. Analysis comparing the untreated cells transfected with siRNA against the scrambled control or CMPK2 was done by using t-tests. *P<0.05; **P<0.01.



Supplementary Figure 2.3: Overexpression of myc-tagged BCL-G in CCR5-U87 cells causes degradation. CCR5-U87 cells were transfected with myc-tagged BCL-G, empty myc-tagged vector, HA-BCL-XL, transfection reagent alone (Lipofectamine) or left untransfected for 48 hours. Western blots showing the protein expression of BCL-G and its degradation products.



Supplementary Figure 2.4: Heatmap Analysis of Top fifty genes Pre-IFN. Heatmap analysis defines the gene clusters seen in the PCA analysis.

CHAPTER III

High-dimensional flow cytometry analysis of T cell responses in individuals who clear multiple reinfections versus remain persistently infected with HCV

Abstract

Hepatitis C virus infects over 70 million people world-wide. During acute infection, infected individuals have two outcomes. Most remain infected and progress to chronic infection, but some individuals spontaneously control infection, and do so repeatedly for multiple infections afterwards. This divergence in infection outcome is in part attributed to differences in virus-specific-T-cell responses. In particular, HCV-specific CD8+ T-cell effector responses are important for the control of HCV infection. However, the phenotypes of these cells are not fully defined. To address this question, we developed a 28-color/30-parameter flow cytometry panel to simultaneously assess multiple inhibitory markers, chemokine receptors, and other phenotypic markers. This panel is the most comprehensive panel focused on T-cells to date and evaluates the differences in phenotypic marker expression in patients who spontaneously control infection compared to those who remain chronically infected. The overall goal of this panel is to fully understand the differences in HCV-specific CD8+ T-cells that render them efficient in naturally controlling HCV infection.

Introduction

HCV is a positive-stranded RNA virus that infects more than 70 million people worldwide [95]. This viral infection provides a unique model for understanding the causes of acute versus chronic infection. HCV infection results in progression to chronicity in approximately 75% of individuals and spontaneous clearance in the other 25% of individuals [98]. HCV-specific CD8+ T-cells play an important role in viral clearance through their cytolytic function. Previous studies showed that decreases in both HCV RNA titers and serum levels of alanine aminotransferase (ALT) correlated with CD8+ T-cell response [145-146]. Studies done in chimpanzees

demonstrated that the depletion of CD8+ T-cells prior to HCV challenge resulted in prolonged periods of high viremia. Clearance of HCV was seen once CD8+ T-cells recovered, producing HCV-specific responses [111]. Spontaneous clearance is also associated with sustained HCV-specific CD8+ T-cell responses in both patients and chimpanzees, while chronicity is associated with weak and transient responses [101,112,145, 147]. The functionality of HCV-specific CD8+ T-cells is essential for controlling infection. Functionally impaired T-cells show decreased proliferation, cytolytic activity, and look phenotypically exhausted. This impairment is partially due to the expression of programmed cell death-1 (PD-1), T-cell immunoglobulin and mucin domain-containing molecule (TIM-3), and cytotoxic T-lymphocyte-associated antigen 4 (CTLA-4) [148-152]. However, many questions remain in understanding the complete picture on simultaneous receptor expression on HCV-specific-CD8+ T-cells and the correlation between viral clearance or persistence. Here, we develop a high-parameter flow cytometry panel to fully assess receptor expression of many inhibitory markers including PD-1, CTLA-4, TIM-3, LAG-3, and KLRG1 on antigen specific CD8+ T-cells using HLA Class I multimers. This panel demonstrates differentiation between multiple phenotypic markers in reinfected subjects compared to chronic subjects, providing an essential tool in further understanding the differences in HCV outcome.

Materials and Methods

Study Participants. HCV infected subjects were obtained from the Baltimore Before and After Acute Study of Hepatitis (BBAASH), a longitudinal cohort study of PWID in Baltimore, Maryland. Participants were enrolled in this prospective study if they were at risk for HCV infection and were HCV-antibody negative. Individuals were consented and blood samples were collected

monthly, as previously described [153]. We identified people previously who had sufficient follow-up to evaluate the long-term outcome of infection [99]. HCV RNA testing was performed on plasma or serum samples using the COBAS Taqman RT-PCR quantitative assay (Roche).

Defining Chronic and Reinfected Participants. HCV spontaneous controllers were previously defined [153] as individuals who were HCV RNA negative but HCV antibody positive for at least 60 days. Chronic infection was defined by periods of continuous viremia with the same virus. Reinfection was defined by having new genetically unique periods of viremia, as defined by Core-E1 assay, in HCV spontaneous controllers. Subsequent reinfections were defined by having undetectable HCV RNA levels for at least 60 days.

IFN- γ -ELISpot Assay. HCV-specific CD8+ T-cell responses were identified using the interferon-gamma (IFN- γ) ELISpot assay as previously described [154]. PBMC from participants were screened for the recognition of HCV-specific antigens using the previously described optimal HCV epitopes as well as pools of overlapping peptides.

Flow Cytometry Staining Protocol.

1. Thaw cryopreserved PBMCs with thawing medium (R50) using the drip method. Briefly, warm cryovials at 37°C in water for about 1 minute until frozen cells release from the bottom of the cryovial. Slowly drip 1mL of pre-warmed R50 into the cryovial and transfer to 15mL conical. Slowly drip 2mL R50, rest 1 minute, and continue until cells are resuspended in 15mL R50.
2. Centrifuge cells 400 x g for 5 minutes
3. Discard supernatant and wash cells once in chilled PBS

4. Centrifuge cells 400 x g for 5 minutes
5. Resuspend cells in 100uL Live/Dead Blue (diluted 1:200 in PBS) and transfer cells to 96-well V-bottom plate.
6. Incubate 20 min at 4°C in the dark
7. Bring staining reactions to 200uL with PBS
8. Centrifuge cells 400 x g for 5 min
9. Discard supernatant and wash cells twice with chilled FACS (0.5%BSA in PBS) buffer
10. Bring samples up in 100uL and add 1 ul of FC block to all samples
11. Incubate for 10 min at room temp
12. Bring staining reactions to 200uL with FACS buffer
13. Centrifuge cells 400 x g for 5 min
14. Discard supernatant and wash cells once with chilled FACS buffer
15. Bring staining reactions to 100uL with FACS buffer
16. Add 2 ul of unlabeled pentamer to the appropriate tube
17. Incubate for 10 min on ice
18. Wash cells once with FACS buffer and discard supernatant
19. Add 8ul of APC flourotag to cells
20. Incubate for 20 min on ice
21. Wash cells once with FACS buffer and discard supernatant
22. Resuspend cells in 100uL staining medium containing antibodies (**Table 1**)
23. Incubate for 30 min at 4°C in the dark
24. Bring staining reactions to 200uL with FACS buffer

25. Centrifuge cells 400 x g for 5 min
26. Discard supernatant and wash cells twice with FACS buffer
27. Discard supernatant and fix cells using 100uL eBioscience FoxP3 Fix/Perm buffer
28. Incubate 20 minutes on ice in the dark
29. Add 100uL of eBioscience FoxP3 Perm/Wash buffer to wash
30. Centrifuge cells 2000 rpm for 5 minutes
31. Make intracellular staining (ICS) antibody cocktail mix
32. Discard supernatant and immediately add 100uL of ICS antibody cocktail mix
33. Incubate for 20-30 minutes on ice in the dark
34. Add 100uL Perm/Wash buffer to staining reactions to wash
35. Wash cells 2x times and discard supernatant
36. Bring reactions to 200uL with FACS buffer
37. Acquire samples on X50 cytometer at the NIH

Flow Cytometry Analysis.

All statistical analysis was done using Flowjo version 10 software of all FCS files. Briefly, we manually gated all T cells subsets, including antigen-specific CD8+ T-cell subsets. We then concatenate all downsampled samples together to run UMAP dimensional reduction analysis to identify populations that cluster (indication of similarity) and assess heat maps for phenotypes of these clusters.

Results

Panel Development. Our aim was to develop a panel that encompassed phenotypic markers that could be important to understanding HCV pathogenesis. To do so, we added 27 markers

that have previously been described to be important for HCV outcome and differentiating T-cell subsets (**Table 3.1**). Optimization of a comprehensive panel involved antibody titrations to determine the appropriate dilution in which the negative and positive populations were clearly differentiated (**Table 3.1**). Examples of two antibody titrations included in panel development are shown in **Supplementary Figure 3.1**. After many iterations of our panel, the final developed panel is pictured in **Figure 3.1A** as an N by N plot. This plot is used to visualize every marker in the panel against one another to differentiate any spillover that would cause compensation issues. Our final panel has minimal spillover and compensation issues.

Identification of HCV Subjects. The overall goal of the panel was to allow simultaneous analysis of multiple interesting markers on HCV-specific T-cells. We used three different class I pentamers to study the HCV-specific CD8⁺ T-cell responses in one subject who progresses to chronic infection (S29), and one subject who repeatedly clears infection (S553). Both S29 and S553 are PWID enrolled in the BBAASH cohort, who were longitudinally followed for over six years. S29 was chosen as our chronic control because he is infected with a genotype 1a strain and remained chronically infected for over six years (**Figure 3.2A**). S29 was sampled frequently during both acute and chronic infection. In comparison, S553 was acutely infected with a genotype 1b virus, but clears infection. S553 is infected with a 1a infection and then 3a infection before clearing their second infection. It is possible S553 cleared the 1a infection prior to being infected with a 3a genotype, but infrequent sampling made it difficult to deduce. S553 goes on to clear a genetically distinct 1a infection, and two genetically distinct 2b infections (**Figure 3.2B**).

Using the IFN- γ -ELISpot assay we determined peptides recognized by CD8+ T cells at multiple sampling visits for both S29 and S553, and designed pentamers using the sequences recognized as listed in **Table 3.2**. Our progressive gating strategy (**Figure 3.3A**), demonstrates steps taken to clearly differentiate the effector memory (TEM), central memory (TCM), naïve (TN), and the CD45RA+ effector memory (TEMRA) CD8+ T-cell subsets. Both S29 and S553 had HCV-specific CD8+ T-cell responses, and gating was based on a healthy control to eliminate any non-specific background staining (**Figure 3.3B**). Pentamer staining for the other time points are visualized in **Supplementary Figure 3.2**.

High-Parameter flow Analysis of HCV-Specific CD8+ T-cells in HCV Subjects. Given the multiple parameters used to assess differences we performed an unbiased high dimensional analysis known as UMAP. Briefly, UMAPs are used to show flow populations that are similar to each other, and therefore cluster together. Heat map analysis was performed to globally highlight specific markers that were highly expressed in different clusters (**Figure 3.4A**). S29 clustered separately from S553, but interestingly the different time points assayed for S553 clustered separately as well. The UMAP heatmap analysis revealed the S29 cluster had higher expression of PD-1, TCF1, and CD38 than the S553 clusters, while the S553 T3 cluster had higher expression of CD127, Tigit, and CXCR3. We further assessed the expression of common inhibitory markers within our HCV-specific CD8+ T-cells, using median mean fluorescence intensities (MFI) (**Figure 3.4B-D**). MFI is a useful tool to assess mean fluorescence intensities when there are no clear positive and negative populations. PD-1 can have varying degrees of intensities as visualized in **Figure 3.4B**. PD-1, TCF1, and Tigit were expressed at varying degrees across all time points in both S29 and S553. For example, S29 T1 (light red histograms) had high levels of TCF1, Tigit, and

PD-1, whereas S553 T2 (orange histogram) had low levels of PD-1, intermediate levels of Tigit, and high levels of TCF1 expression (**Figure 3.4B-D**). There was no significant difference in expression of Tim-3, LAG-3, and KLRG1 across both subjects and all time points (**Supplementary Figure 3.3**).

Next, we assessed the PD-1 and CTLA-4 expression in HCV-specific CD8+ T-cells for S29 T2 and S553 T3. These time points were chosen because they had the largest cluster of pentamer staining to allow differentiation of markers, and were both in the chronic phase of infection. All HCV-specific CD8+ T-cells in S29 were PD-1 positive and CTLA-4 negative, while all HCV-specific CD8+ T-cells in S553 were PD-1 and CTLA-4 double negative (**Figure 3.5A-B**). We then assessed the activation state of HCV-specific CD8+ T-cells by expression of CD38 and found S29 had high expression of CD38, whereas S553 had low expression of CD38 (**Figure 3.5C-D**). Antigen-specific CD8+ T-cells in S29 expressed low levels of CD127, in comparison to S553 which expressed high levels of CD127. Finally, both S29 and S553 had high expression of pentamer positive cells in the effector memory population (**Figure 3.5E-F**). S553 also had higher expression of pentamer positive cells in the TEMRA subset in comparison to S29 (**Supplementary Figure 3.4**).

Discussion and Limitations

HCV remains to be a major public health issue as rates of HCV infection are increasing. Although there is a cure for HCV, a prophylactic vaccine has yet to be developed. The need for a vaccine is evident with the high costs of treatment, downstream health complications from chronic infection, and the low number of individuals being tested for HCV. Natural infection with HCV results in two major outcomes; an individual remains chronically infected or an individual clears infection. Given this phenomenon, studying natural HCV infection allows us to understand the

innate and adaptive immune mechanisms needed to result in clearance of infection. HCV-specific CD8+ T-cells play a critical role in clearance as shown previously [111]. Briefly, it was shown that CD8+ T-cell depletion in chimpanzees led to persistence, but restoration of CD8+ T-cells led to rapid clearance of infection. To better characterize human HCV-specific CD8+ T-cells we developed a high parameter flow cytometry panel to simultaneously assess many markers on T-cells, including inhibitory markers, activation markers, and T-cell subset markers. Our developed panel is the most comprehensive flow cytometry panel used in assessing HCV-specific CD8+ T-cells in chronic versus spontaneous clearers. In chronic infection, we demonstrated the upregulation of the inhibitory receptor PD-1. These PD-1 positive HCV-specific T-cells were also low in CD127 expression as previously described in chronic infection with intact antigen [155]. Interestingly, these cells were also high in CD38 expression, a phenotype not usually attributed to impaired function of HCV-specific CD8+ T-cells. Conversely, S553, had low levels of PD-1 expression, and high frequency of CD127 expression on HCV-specific CD8+ T-cells, a phenotype previously reported in individuals who clear infection [156]. A unique population of HCV-specific CD8+ T-cells in S29 had expression of CD127, PD-1, and TCF1, a previously described phenotype in chronic infection consisting of memory-like characteristics with the ability to proliferate [157]. Our panel also revealed unique HCV-specific CD8+ T-cell populations in both S29 and S553. For instance, S553 had PD-1^{lo}, CD127^{hi}, TCF1^{hi}, and CD38^{lo}, CXCR3^{hi} populations that have not previously been reported. This population is unique and could play a role in viral clearance. However, further work needs to be done to assess this relationship.

Development of this panel resulted in limitations, including difficulty detecting OX40 and LAG-3 expression. Multiple clones on multiple fluorophores were tested, before the final antibodies were included in the panel. However, there is still minimal expression of both OX40 and LAG-3 on CD8+ T-cells. This limitation is a result of high-parameter panels in which spill over is inevitable and can make detection of low-expression molecules difficult to detect.

In conclusion, we have developed a high parameter flow cytometry panel to comprehensively assess HCV-specific CD8+ T-cells. This panel identified previously defined populations shown to correlate with clearance or persistence. We have also identified novel HCV-specific CD8+ T-cell populations, but their importance in clearance versus persistence is yet to be studied. Future work involves using this panel to assess additional chronic and spontaneous resolvers to fully understand the T-cell phenotypes essential for clearance. This work is important for vaccine development because it highlights a possible immune mechanism that can be targeted to lead to clearance in HCV naïve individuals.

Tables

Specificity	Dye	Dilution	Function
TCF1	BB515	1:20	T-cell Subset (Precursor memory)
CD11c	BB630	1:160	T-cell Subset (integrin)
TIGIT	BB660	1:80	Co-Inhibitory
CD194 (CCR4)	BB700	1:20	Chemokine involved in cell trafficking of leukocytes
CD185 (CXCR5)	BB790	1:640	Trafficking and marker of Tfh cells
CD223 (LAG-3)	BV421	1:20	Co-Inhibitory
CD8	BV510	1:160	Lineage
CD28	BV570	1:20	Co-Stimulatory
CD161	BV605	1:40	T-cell Subset and NK cell function
HLADR	BV650	1:80	Activation
CD134 (OX40)	BV711	1:1	Co-Stimulatory
CD38	BV750	1:40	Activation
CD27	BV785	1:160	Activation
CD197 (CCR7)	BUV395	1:20	T-cell Homing to secondary lymphoid organs
Amine-Reactive	LIVE/DEAD Blue	1:20	Viability
CD3	BUV496	1:80	Lineage
CD25	BUV563	1:160	Lineage
CD279 (PD-1)	BUV661	1:20	Co-Inhibitory
CD366 (TIM-3)	BUV737	1:20	Co-Inhibitory
CD4	BUV805	1:20	Lineage
Pentamer	APC	1:20	Antigen-Specificity
CCR5	Ax700	1:40	T-cell Homing
CD45RA	APC Cy7	1:320	Lineage
CD183 (CXCR3)	PE	2:1	Trafficking
KLRG1	PE-CF594	1:20	Co-Inhibitory
CD127 (IL-7R α)	PE-Cy5	1:1	Differentiation and memory marker on T-cells
CD152 (CTLA-4)	PE-Cy7	1:20	Co-Inhibitory

Table 3.1: The Optimized 27-color Panel for Flow Cytometry. Dilutions for each marker were determined and optimized so each marker in this panel was appropriately expressed, with minimal spillover. The fluorophore and function of each marker are listed above.

Subject	Days post-infection	Pentamer Sequence	Time Point
29	58	CINGVCWTV	S29 T1
	1524	CINGVCWTV	S29 T2
553	1232	CINGVCWTV	S553 T1
	1232	HSKKKCDEL	S553 T2
	1597	ATDALMTGY	S553 T3
	2003	ATDALMTGY	S553 T4

Table 3.2: Summary of Subjects and Pentamer Sequence Used for Flow Cytometry. S29

(chronic) and S553 (reinfected) were selected for our preliminary studies. The pentamer sequenced used, the days post initial infection, and the time point label are listed.

Figures

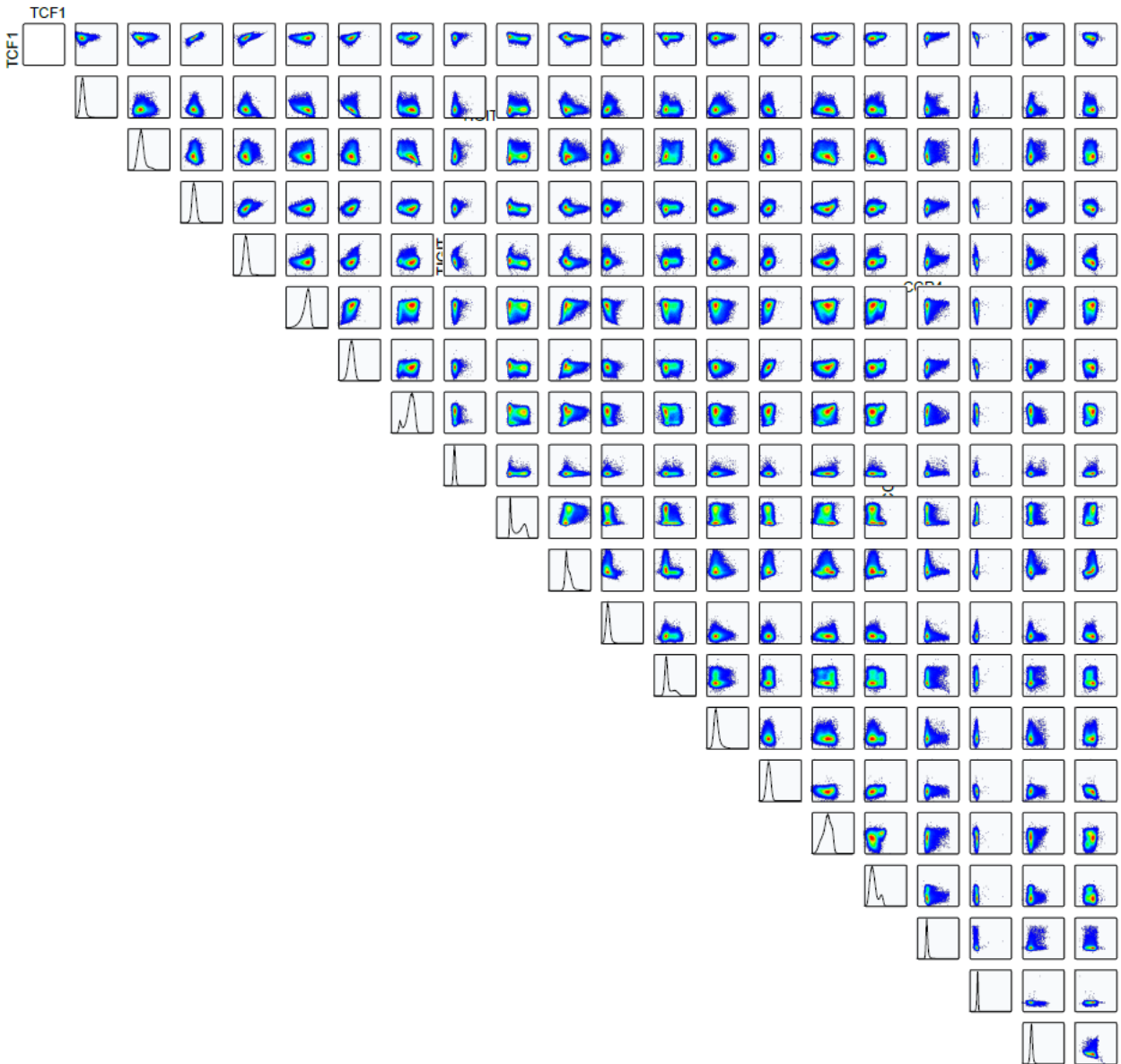


Figure 3.1A: N by N plot of All Markers in 27-Color Flow Panel. NxN plot showing every parameter against each other in the developed panel. Note that there are distinct populations with minimal spill over into other channels.

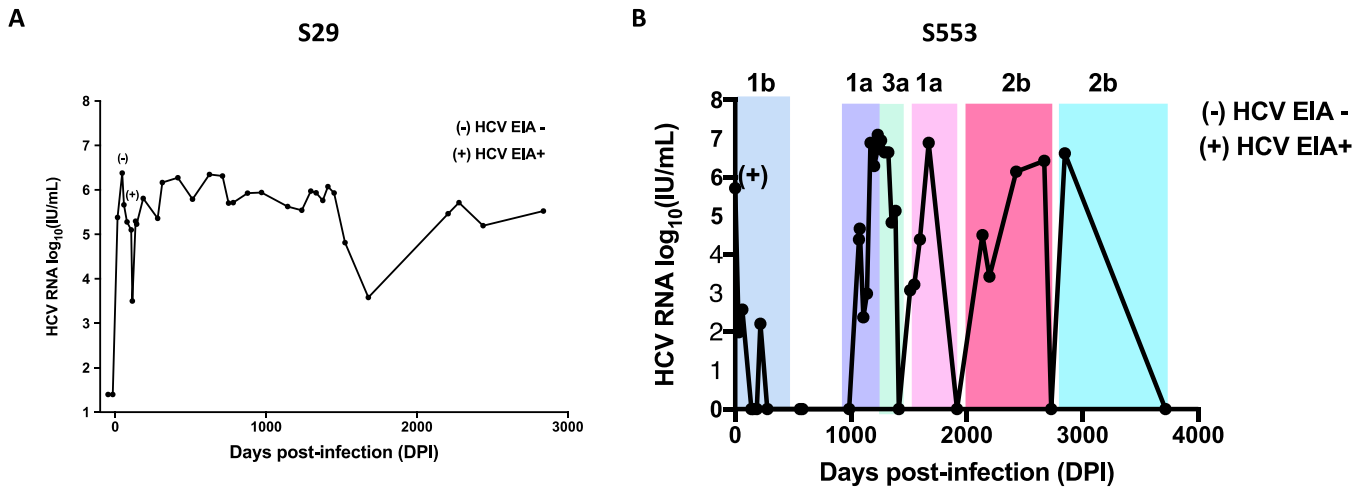


Figure 3.2: Representative graphs demonstrating the longitudinal history of viremia in subjects S29 and S553. A) Log transformed HCV RNA levels are graphed for S29, who remains chronically infected with genotype 1a virus for over six years. **B)** Log transformed HCV RNA levels for S553, who repeatedly clears multiple HCV infections of diverse genotypes over six years. Each genetically unique infection is color coated, as well as the time points S29 and S553 go from antibody negative (-) to antibody positive (+, EIA).

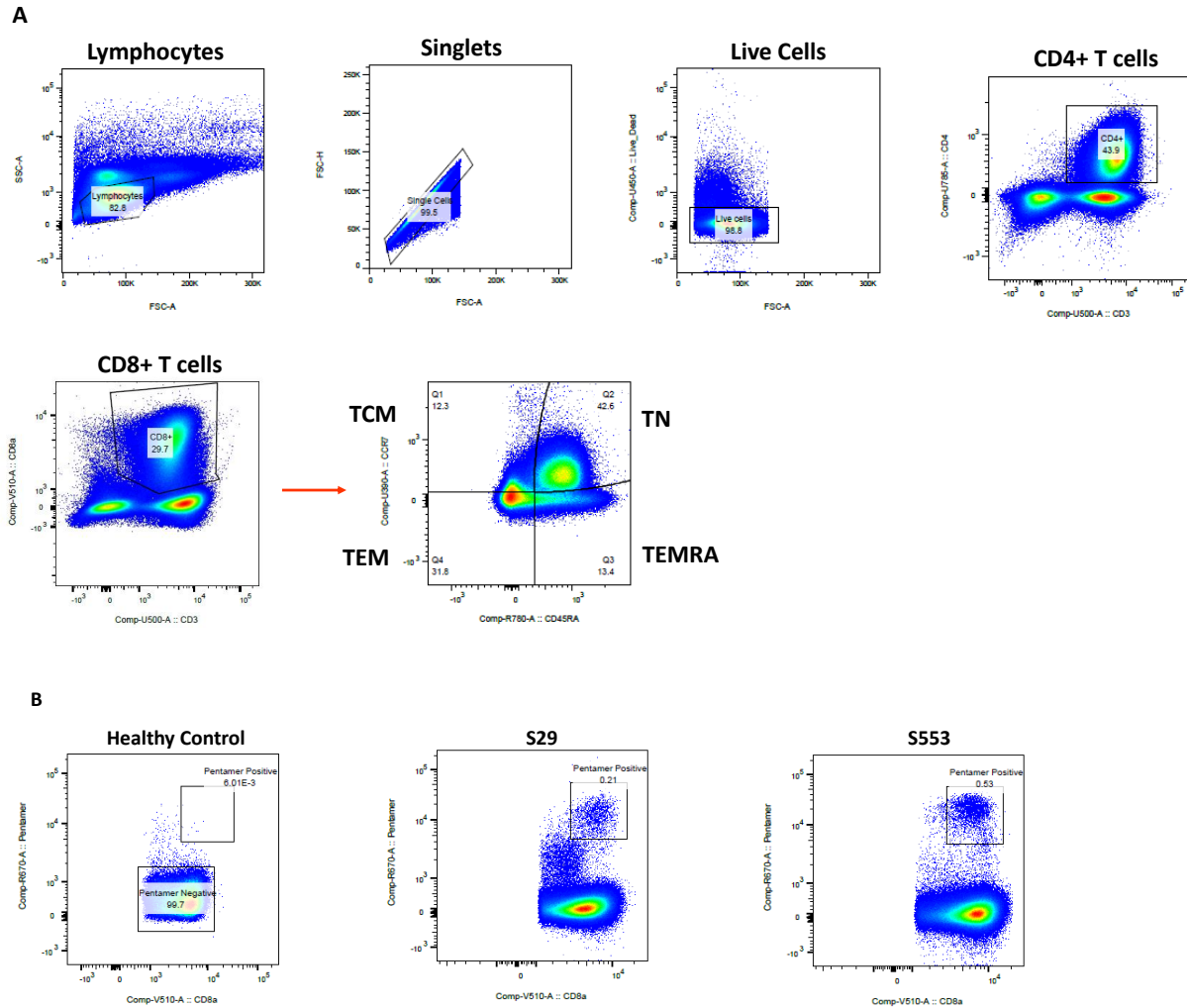


Figure 3.3: Staining Pattern for gating, T-cell differentiation characterization, and identifying HCV-specific CD8+ T-cells. A) Progressive gating strategy to identify CD4+ and CD8+ T-cell populations. Further gating of CD8+ T-cells are shown to identify the major T-cell subsets TCM (central memory), TEM (effector memory), TN (naïve), and TEMRA (CD45RA+ effector memory). **B)** Gating of pentamer-positive CD8+ T-cells to identify a clear antigen positive population in both S29 and S553. A healthy donor was used as a negative control to ensure gating excluded background staining.

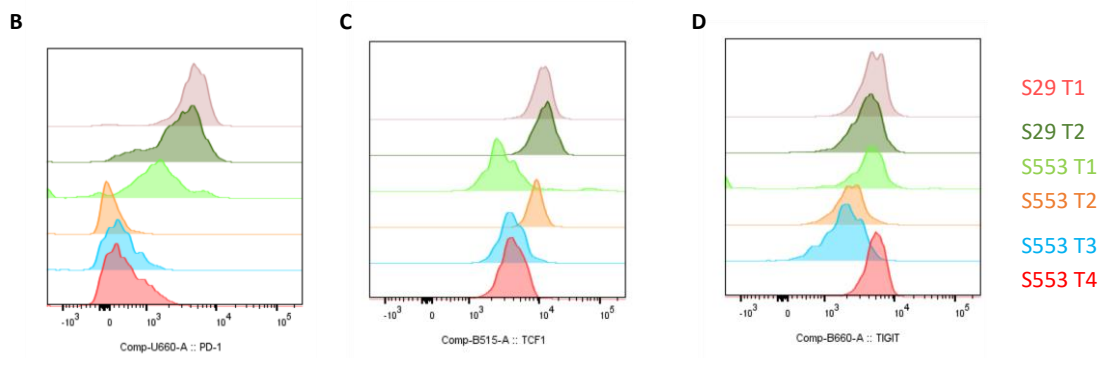
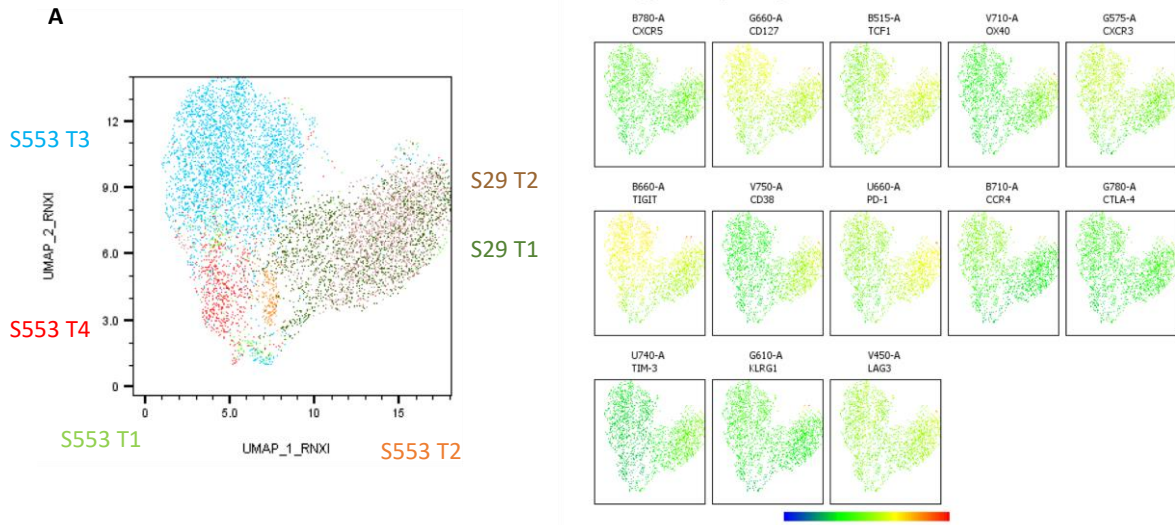


Figure 3.4: High dimensional analysis of HCV-Specific CD8+ T-cells in S29 and S553. **A)** UMAP analysis of HCV-specific CD8+ T-cells in S29 and S553 shows S29 and S553 T-cells cluster separately. T-cells from S29 cluster together through all time points, while S553 cluster separately for most time points indicating phenotypically unique virus-specific populations in each time point. Heatmap analysis shows global expression differences. PD-1, TCF1, and CD38 have higher expression patterns in S29 while CD127, Tigit, and CXCR3 have higher expression patterns in S553. **B)** Median MFI analysis of PD-1, TCF1, and Tigit of HCV-specific CD8+ T-cells. Each time point for S29 and S553 are color coated along with their respective histogram and cluster colors.

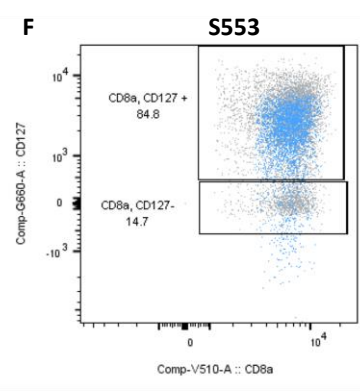
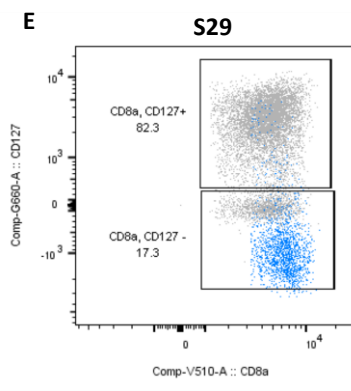
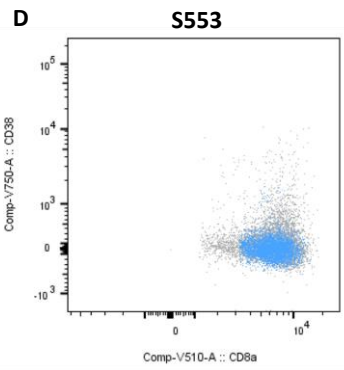
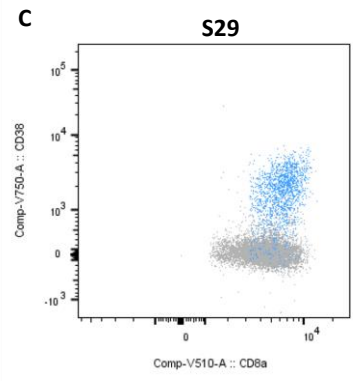
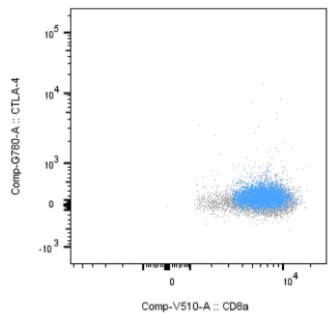
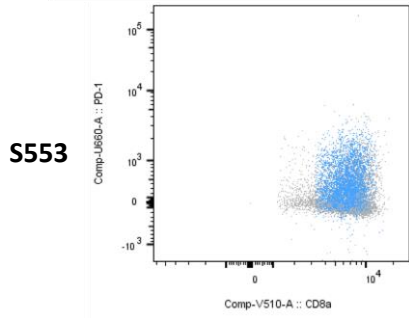
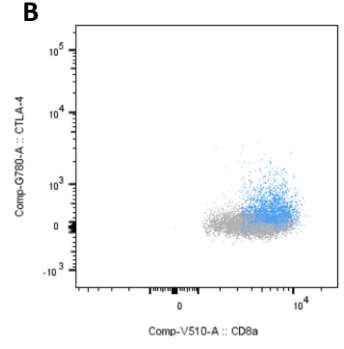
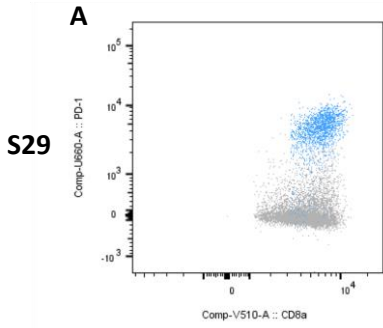
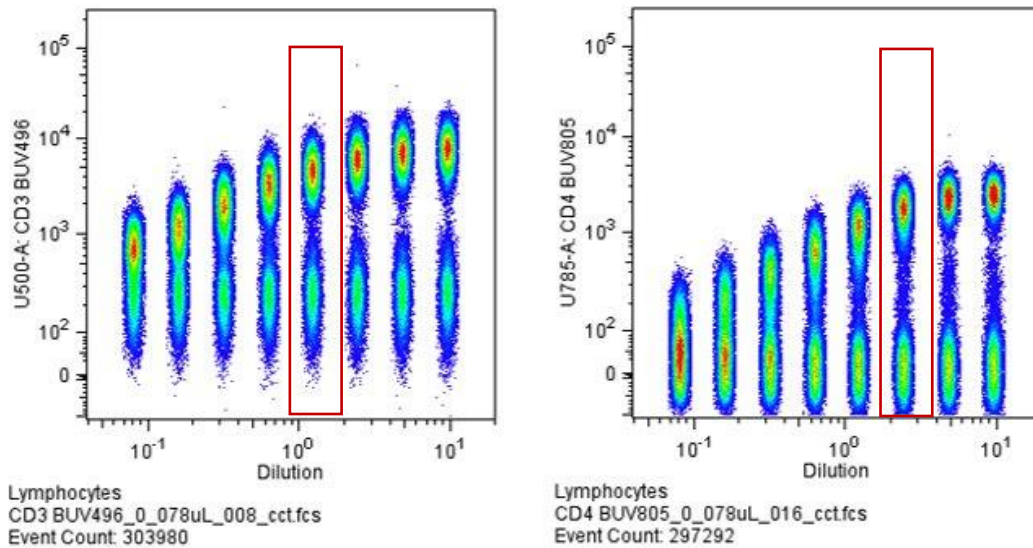
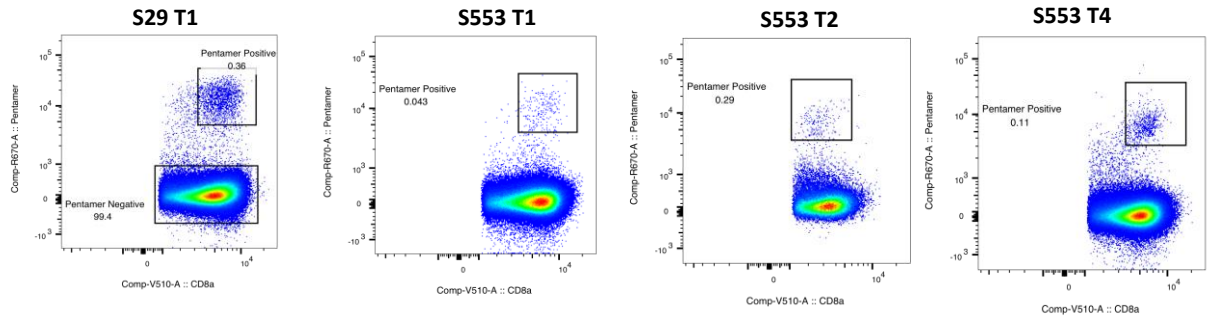


Figure 3.5: HCV-specific CD8+ T-cells diverge in phenotype in S29 and S553. **A)** Expression of PD-1 and **B)** CTLA-4 on HCV-specific CD8+ T-cells. PD-1 was highly expressed on virus-specific CD8+ T-cells in S29. CD38 expression on HCV-specific CD8+ T-cells from **C)** S29 and **D)** S553. CD38 was highly expressed on virus-specific CD8+ T-cells in S29. CD127 expression on HCV-specific CD8+ T-cells from **E)** S29 and **F)** S553. S553 has high expression of CD127 on virus-specific CD8+ T-cells.

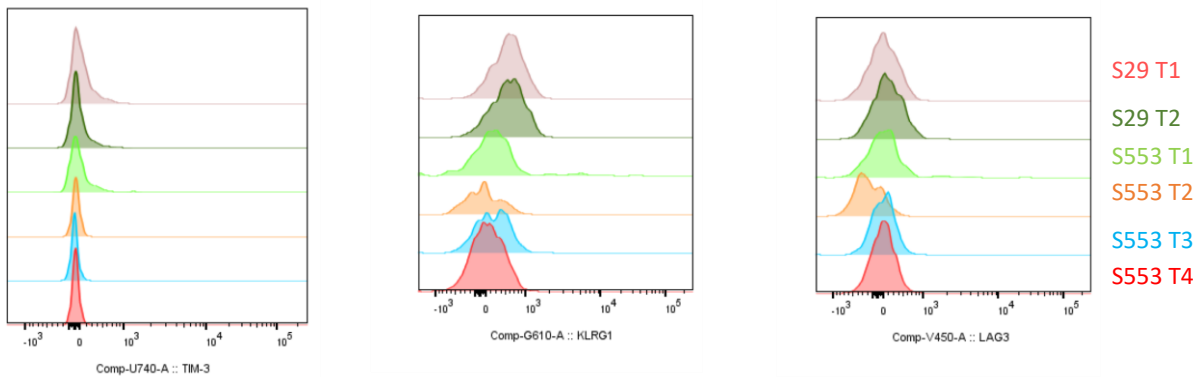
Supplementary Figures



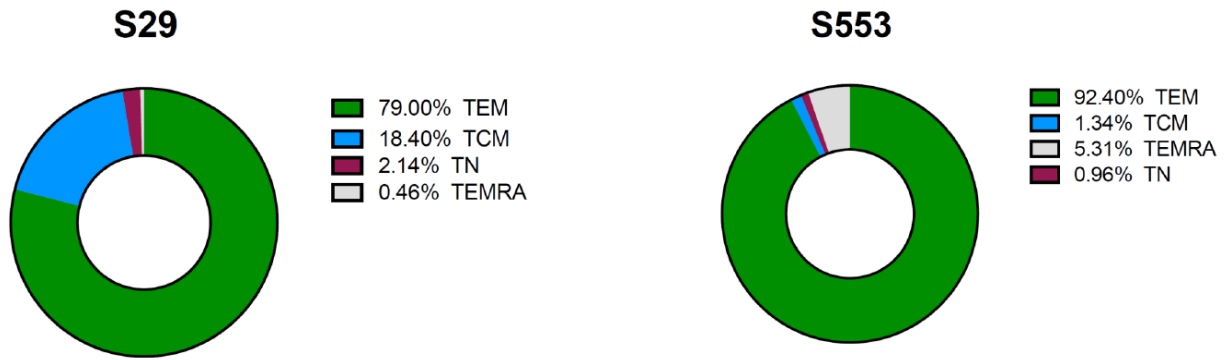
Supplementary Figure 3.1: Titration of CD3 and CD4 for the 27-color Flow Panel. A series of eight 2-fold dilutions were performed on PBMCs stained with CD3 or CD4 flow antibodies. The red box indicates the chosen dilution to include in the panel. 1:20 was chosen for CD4 and 1:40 for CD3.



Supplementary Figure 3.2: HCV-Specific CD8+ T-cells in S29 and S553. Pentamer staining of S29 and S553 at the remaining time points not used in the main analysis. These plots show distinct virus-specific populations on CD8+ T-cells. The black box encompasses the pentamer positive CD8+ T-cells.



Supplementary Figure 3.3: Median MFI of TIM-3, KLRG1, and LAG3 in S29 and S553. HCV-specific CD8+ T-cells were analyzed for expression of TIM-3, KLRG1, and LAG3. All time points were analyzed to show very low expression of all inhibitory markers on virus-specific T-cells. Time points are color-coated with their respective histogram colors.



Supplementary Figure 3.4: HCV-specific CD8⁺ T-cell phenotype in S29 and S553. Pentamer positive CD8⁺ T-cells were analyzed for the characterization in the T-cell subsets EM, CM, TN, and TEMRA. S29 had more virus-specific T-cells with a central memory phenotype, while S553 had more virus-specific T-cells with both the effector memory and TEMRA phenotype. Percentages of total pentamer-positive population in each T-cell subset are shown above.

CHAPTER IV

Conclusions

Conclusions

This thesis presents novel tools to further study immune responses in both HIV-1 and HCV infection in PWIDs that are applicable to a wide variety of viral chronic infections.

In chapter two, we have demonstrated CMPK2 and BCL-G are interferon stimulated genes that restrict HIV-1 infection. RNA interference demonstrated that the anti-HIV-1 effect of IFN α could be attributable to both CMPK2 and BCL2L14. The mechanisms underlying how these ISGs restrict HIV-1 are unknown, but our efforts have led us to better understand both CMPK2 and BCL2L14 in the context of HIV-1 infection. We characterized BCL2L14 as a potential gene that promotes CD4+ T cell decline during HIV-1, due to its relationship with apoptotic proteins. We also identified various genes in the apoptotic pathway, closely correlated with BCL-G expression in HIV-1 positive individuals and persisted after treatment with cART. This research supports the potential use of ISGs and their pathways as targets for small drug therapeutics to control HIV-1 infection, particularly those that inhibit HIV-1 infection before it integrates into the host DNA.

These tools are also applicable to a wide range of viral infections with both CMPK2 and BCL-G as interferon stimulated genes that are putative restriction factors. More broadly BCL-G has a controversial role in apoptosis, and its role in HIV-1 could pose a novel mechanism that explains the CD4+ T-cell decline that is seen in the natural progression of HIV-1 infection.

In chapter three, we developed a novel high-parameter flow cytometry panel to longitudinally assess the differences in antigen-specific T cells in individuals who naturally clear infection multiple times, in comparison to those who fail to do so. Since the release of directly acting antiviral agents (DAAs), HCV can be cured, but many factors limit the effectiveness of

DAA's in eradicating HCV. As a result, the development of a prophylactic vaccine is critical for efforts towards eradicating HCV. Vaccine development has been complicated by the wide genetic variability of HCV and the limited characterization of cellular responses important in controlling infection. Given the importance of CD4+ and CD8+ HCV-specific T-cell responses in controlling HCV in individuals who become reinfected, better understanding of these T-cell responses will help guide effective vaccine design. It is likely that a combination of multiple phenotypic markers contributes to the difference in T-cells that either mount control or fail to elicit a protective immune response. However, it is unclear which markers and if any in combination are the key in control of HCV infection. This research highlights the importance of T-cells in understanding clearance of human HCV infection, and hopes to inform HCV vaccine design.

REFERENCES

1. Iwasaki A, Medzhitov R. Control of adaptive immunity by the innate immune system. *Nature immunology*. 2015;16(4):343-53. doi:10.1038/ni.3123.
2. Brubaker SW, Bonham KS, Zanoni I, Kagan JC. Innate immune pattern recognition: a cell biological perspective. *Annual review of immunology*. 2015;33:257-90. doi:10.1146/annurev-immunol-032414-112240.
3. van Montfoort N, Olganier D, Hiscott J. Unmasking immune sensing of retroviruses: interplay between innate sensors and host effectors. *Cytokine & growth factor reviews*. 2014;25(6):657-68. doi:10.1016/j.cytogfr.2014.08.006.
4. Collins SE, Mossman KL. Danger, diversity and priming in innate antiviral immunity. *Cytokine & growth factor reviews*. 2014;25(5):525-31. doi:10.1016/j.cytogfr.2014.07.002.
5. Silvin A, Manel N. Innate immune sensing of HIV infection. *Current opinion in immunology*. 2015;32:54-60. doi:10.1016/j.coi.2014.12.003.
6. McNab F, Mayer-Barber K, Sher A, Wack A, O'Garra A. Type I interferons in infectious disease. *Nature reviews Immunology*. 2015;15(2):87-103. doi:10.1038/nri3787.
7. Diamond MS, Farzan M. The broad-spectrum antiviral functions of IFIT and IFITM proteins. *Nature reviews Immunology*. 2013;13(1):46-57. doi:10.1038/nri3344.
8. Brass AL, Huang IC, Benita Y, John SP, Krishnan MN, Feeley EM et al. The IFITM proteins mediate cellular resistance to influenza A H1N1 virus, West Nile virus, and dengue virus. *Cell*. 2009;139(7):1243-54. doi:10.1016/j.cell.2009.12.017.
9. Lu J, Pan Q, Rong L, He W, Liu SL, Liang C. The IFITM proteins inhibit HIV-1 infection. *Journal of virology*. 2011;85(5):2126-37. doi:10.1128/JVI.01531-10.

10. Feeley EM, Sims JS, John SP, Chin CR, Pertel T, Chen LM et al. IFITM3 inhibits influenza A virus infection by preventing cytosolic entry. *PLoS pathogens*. 2011;7(10):e1002337. doi:10.1371/journal.ppat.1002337.
11. Weston S, Czieso S, White IJ, Smith SE, Wash RS, Diaz-Soria C et al. Alphavirus Restriction by IFITM Proteins. *Traffic*. 2016;17(9):997-1013. doi:10.1111/tra.12416.
12. Chernomordik LV, Kozlov MM. Membrane hemifusion: crossing a chasm in two leaps. *Cell*. 2005;123(3):375-82. doi:10.1016/j.cell.2005.10.015.
13. Li K, Markosyan RM, Zheng YM, Golfetto O, Bungart B, Li M et al. IFITM proteins restrict viral membrane hemifusion. *PLoS pathogens*. 2013;9(1):e1003124. doi:10.1371/journal.ppat.1003124.
14. Garg H, Viard M, Jacobs A, Blumenthal R. Targeting HIV-1 gp41-induced fusion and pathogenesis for anti-viral therapy. *Current topics in medicinal chemistry*. 2011;11(24):2947-58.
15. Compton AA, Bruel T, Porrot F, Mallet A, Sachse M, Euvrard M et al. IFITM proteins incorporated into HIV-1 virions impair viral fusion and spread. *Cell host & microbe*. 2014;16(6):736-47. doi:10.1016/j.chom.2014.11.001. *A paper showing a mechanism in which IFITM incorporates itself into virions to block fusion.*
16. Yu J, Li M, Wilkins J, Ding S, Swartz TH, Esposito AM et al. IFITM Proteins Restrict HIV-1 Infection by Antagonizing the Envelope Glycoprotein. *Cell reports*. 2015;13(1):145-56. doi:10.1016/j.celrep.2015.08.055. *A paper showing how IFITM acts by inhibiting production and incorporation of envelope proteins.*

17. Foster TL, Wilson H, Iyer SS, Coss K, Doores K, Smith S et al. Resistance of Transmitted Founder HIV-1 to IFITM-Mediated Restriction. *Cell host & microbe*. 2016.
doi:10.1016/j.chom.2016.08.006.
18. Stremlau M, Owens CM, Perron MJ, Kiessling M, Autissier P, Sodroski J. The cytoplasmic body component TRIM5alpha restricts HIV-1 infection in Old World monkeys. *Nature*. 2004;427(6977):848-53. doi:10.1038/nature02343.
19. Nisole S, Stoye JP, Saib A. TRIM family proteins: retroviral restriction and antiviral defence. *Nature reviews Microbiology*. 2005;3(10):799-808. doi:10.1038/nrmicro1248.
20. Han K, Lou DI, Sawyer SL. Identification of a genomic reservoir for new TRIM genes in primate genomes. *PLoS genetics*. 2011;7(12):e1002388. doi:10.1371/journal.pgen.1002388.
21. Zhang F, Hatzioannou T, Perez-Caballero D, Derse D, Bieniasz PD. Antiretroviral potential of human tripartite motif-5 and related proteins. *Virology*. 2006;353(2):396-409.
doi:10.1016/j.virol.2006.05.035.
22. Battivelli E, Lecossier D, Matsuoka S, Migraine J, Clavel F, Hance AJ. Strain-specific differences in the impact of human TRIM5alpha, different TRIM5alpha alleles, and the inhibition of capsid-cyclophilin A interactions on the infectivity of HIV-1. *Journal of virology*. 2010;84(21):11010-9. doi:10.1128/JVI.00758-10.
23. Soll SJ, Wilson SJ, Kutluay SB, Hatzioannou T, Bieniasz PD. Assisted evolution enables HIV-1 to overcome a high TRIM5alpha-imposed genetic barrier to rhesus macaque tropism. *PLoS pathogens*. 2013;9(9):e1003667. doi:10.1371/journal.ppat.1003667.

24. Li X, Gold B, O'Huigin C, Diaz-Griffero F, Song B, Si Z et al. Unique features of TRIM5alpha among closely related human TRIM family members. *Virology*. 2007;360(2):419-33. doi:10.1016/j.virol.2006.10.035.
25. Kutluay SB, Perez-Caballero D, Bieniasz PD. Fates of retroviral core components during unrestricted and TRIM5-restricted infection. *PLoS pathogens*. 2013;9(3):e1003214. doi:10.1371/journal.ppat.1003214.
26. Mandell MA, Kimura T, Jain A, Johansen T, Deretic V. TRIM proteins regulate autophagy: TRIM5 is a selective autophagy receptor mediating HIV-1 restriction. *Autophagy*. 2014;10(12):2387-8. doi:10.4161/15548627.2014.984278.
27. Pertel T, Hausmann S, Morger D, Zuger S, Guerra J, Lascano J et al. TRIM5 is an innate immune sensor for the retrovirus capsid lattice. *Nature*. 2011;472(7343):361-5. doi:10.1038/nature09976.
28. Nepveu-Traversy ME, Berthoux L. The conserved sumoylation consensus site in TRIM5alpha modulates its immune activation functions. *Virus research*. 2014;184:30-8. doi:10.1016/j.virusres.2014.02.013.
29. Campbell EM, Weingart J, Sette P, Opp S, Sastri J, O'Connor SK et al. TRIM5alpha-Mediated Ubiquitin Chain Conjugation Is Required for Inhibition of HIV-1 Reverse Transcription and Capsid Destabilization. *Journal of virology*. 2016;90(4):1849-57. doi:10.1128/JVI.01948-15.
30. Barr SD, Smiley JR, Bushman FD. The interferon response inhibits HIV particle production by induction of TRIM22. *PLoS pathogens*. 2008;4(2):e1000007. doi:10.1371/journal.ppat.1000007.

31. Singh R, Gaiha G, Werner L, McKim K, Mlisana K, Luban J et al. Association of TRIM22 with the type 1 interferon response and viral control during primary HIV-1 infection. *Journal of virology*. 2011;85(1):208-16. doi:10.1128/JVI.01810-10.
32. Kajaste-Rudnitski A, Marelli SS, Pultrone C, Pertel T, Uchil PD, Mechti N et al. TRIM22 inhibits HIV-1 transcription independently of its E3 ubiquitin ligase activity, Tat, and NF-kappaB-responsive long terminal repeat elements. *Journal of virology*. 2011;85(10):5183-96. doi:10.1128/JVI.02302-10.
33. Turrini F, Marelli S, Kajaste-Rudnitski A, Lusic M, Van Lint C, Das AT et al. HIV-1 transcriptional silencing caused by TRIM22 inhibition of Sp1 binding to the viral promoter. *Retrovirology*. 2015;12:104. doi:10.1186/s12977-015-0230-0. *A paper showing the mechanism in which TRIM22 inhibits HIV-1 LTR transcriptional activation by inhibition of Sp1.*
34. Setiawan LC, Kootstra NA. Adaptation of HIV-1 to rhTrim5alpha-mediated restriction in vitro. *Virology*. 2015;486:239-47. doi:10.1016/j.virol.2015.09.017.
35. Nakayama EE, Shioda T. Impact of TRIM5alpha in vivo. *AIDS*. 2015;29(14):1733-43. doi:10.1097/QAD.0000000000000812.
36. Laguette N, Sobhian B, Casartelli N, Ringeard M, Chable-Bessia C, Segeral E et al. SAMHD1 is the dendritic- and myeloid-cell-specific HIV-1 restriction factor counteracted by Vpx. *Nature*. 2011;474(7353):654-7. doi:10.1038/nature10117.
37. Hrecka K, Hao C, Gierszewska M, Swanson SK, Kesik-Brodacka M, Srivastava S et al. Vpx relieves inhibition of HIV-1 infection of macrophages mediated by the SAMHD1 protein. *Nature*. 2011;474(7353):658-61. doi:10.1038/nature10195.

38. Descours B, Cribier A, Chable-Bessia C, Ayinde D, Rice G, Crow Y et al. SAMHD1 restricts HIV-1 reverse transcription in quiescent CD4(+) T-cells. *Retrovirology*. 2012;9:87. doi:10.1186/1742-4690-9-87.
39. Baldauf HM, Pan X, Erikson E, Schmidt S, Daddacha W, Burggraf M et al. SAMHD1 restricts HIV-1 infection in resting CD4(+) T cells. *Nature medicine*. 2012;18(11):1682-7. doi:10.1038/nm.2964.
40. St Gelais C, de Silva S, Amie SM, Coleman CM, Hoy H, Hollenbaugh JA et al. SAMHD1 restricts HIV-1 infection in dendritic cells (DCs) by dNTP depletion, but its expression in DCs and primary CD4+ T-lymphocytes cannot be upregulated by interferons. *Retrovirology*. 2012;9:105. doi:10.1186/1742-4690-9-105.
41. Ahn J. Functional organization of human SAMHD1 and mechanisms of HIV-1 restriction. *Biological chemistry*. 2016;397(4):373-9. doi:10.1515/hsz-2015-0260.
42. Goldstone DC, Ennis-Adeniran V, Hedden JJ, Groom HC, Rice GI, Christodoulou E et al. HIV-1 restriction factor SAMHD1 is a deoxynucleoside triphosphate triphosphohydrolase. *Nature*. 2011;480(7377):379-82. doi:10.1038/nature10623.
43. Lahouassa H, Daddacha W, Hofmann H, Ayinde D, Logue EC, Dragin L et al. SAMHD1 restricts the replication of human immunodeficiency virus type 1 by depleting the intracellular pool of deoxynucleoside triphosphates. *Nature immunology*. 2012;13(3):223-8. doi:10.1038/ni.2236.
44. Powell RD, Holland PJ, Hollis T, Perrino FW. Aicardi-Goutieres syndrome gene and HIV-1 restriction factor SAMHD1 is a dGTP-regulated deoxynucleotide triphosphohydrolase. *The Journal of biological chemistry*. 2011;286(51):43596-600. doi:10.1074/jbc.C111.317628.

45. Tang C, Ji X, Wu L, Xiong Y. Impaired dNTPase activity of SAMHD1 by phosphomimetic mutation of Thr-592. *The Journal of biological chemistry*. 2015;290(44):26352-9. doi:10.1074/jbc.M115.677435.
46. Rehwinkel J, Maelfait J, Bridgeman A, Rigby R, Hayward B, Liberatore RA et al. SAMHD1-dependent retroviral control and escape in mice. *The EMBO journal*. 2013;32(18):2454-62. doi:10.1038/emboj.2013.163.
47. Kim B, Nguyen LA, Daddacha W, Hollenbaugh JA. Tight interplay among SAMHD1 protein level, cellular dNTP levels, and HIV-1 proviral DNA synthesis kinetics in human primary monocyte-derived macrophages. *The Journal of biological chemistry*. 2012;287(26):21570-4. doi:10.1074/jbc.C112.374843.
48. Bonifati S, Daly MB, St Gelais C, Kim SH, Hollenbaugh JA, Shepard C et al. SAMHD1 controls cell cycle status, apoptosis and HIV-1 infection in monocytic THP-1 cells. *Virology*. 2016;495:92-100. doi:10.1016/j.virol.2016.05.002.
49. Beloglazova N, Flick R, Tchigvintsev A, Brown G, Popovic A, Nocek B et al. Nuclease activity of the human SAMHD1 protein implicated in the Aicardi-Goutieres syndrome and HIV-1 restriction. *The Journal of biological chemistry*. 2013;288(12):8101-10. doi:10.1074/jbc.M112.431148.
50. Ryoo J, Choi J, Oh C, Kim S, Seo M, Kim SY et al. The ribonuclease activity of SAMHD1 is required for HIV-1 restriction. *Nature medicine*. 2014;20(8):936-41. doi:10.1038/nm.3626. *A paper showing that SAMHD1 also needs its RNase activity to inhibit HIV-1 and not just its ability to deplete dNTP levels.*

51. Kyei GB, Cheng X, Ramani R, Ratner L. Cyclin L2 is a critical HIV dependency factor in macrophages that controls SAMHD1 abundance. *Cell host & microbe*. 2015;17(1):98-106. doi:10.1016/j.chom.2014.11.009.
52. Berger A, Sommer AF, Zwarg J, Hamdorf M, Welzel K, Esly N et al. SAMHD1-deficient CD14+ cells from individuals with Aicardi-Goutieres syndrome are highly susceptible to HIV-1 infection. *PLoS pathogens*. 2011;7(12):e1002425. doi:10.1371/journal.ppat.1002425.
53. Harris RS, Dudley JP. APOBECs and virus restriction. *Virology*. 2015;479-480:131-45. doi:10.1016/j.virol.2015.03.012.
54. Stavrou S, Ross SR. APOBEC3 Proteins in Viral Immunity. *J Immunol*. 2015;195(10):4565-70. doi:10.4049/jimmunol.1501504.
55. Koning FA, Newman EN, Kim EY, Kunstman KJ, Wolinsky SM, Malim MH. Defining APOBEC3 expression patterns in human tissues and hematopoietic cell subsets. *Journal of virology*. 2009;83(18):9474-85. doi:10.1128/JVI.01089-09.
56. Gillick K, Pollpeter D, Phalora P, Kim EY, Wolinsky SM, Malim MH. Suppression of HIV-1 infection by APOBEC3 proteins in primary human CD4(+) T cells is associated with inhibition of processive reverse transcription as well as excessive cytidine deamination. *Journal of virology*. 2013;87(3):1508-17. doi:10.1128/JVI.02587-12.
57. Chaipan C, Smith JL, Hu WS, Pathak VK. APOBEC3G restricts HIV-1 to a greater extent than APOBEC3F and APOBEC3DE in human primary CD4+ T cells and macrophages. *Journal of virology*. 2013;87(1):444-53. doi:10.1128/JVI.00676-12.
58. Harris RS, Bishop KN, Sheehy AM, Craig HM, Petersen-Mahrt SK, Watt IN et al. DNA deamination mediates innate immunity to retroviral infection. *Cell*. 2003;113(6):803-9.

59. Bishop KN, Holmes RK, Sheehy AM, Davidson NO, Cho SJ, Malim MH. Cytidine deamination of retroviral DNA by diverse APOBEC proteins. *Current biology : CB.* 2004;14(15):1392-6. doi:10.1016/j.cub.2004.06.057.
60. Mangeat B, Turelli P, Caron G, Friedli M, Perrin L, Trono D. Broad antiretroviral defence by human APOBEC3G through lethal editing of nascent reverse transcripts. *Nature.* 2003;424(6944):99-103. doi:10.1038/nature01709.
61. Casartelli N, Guivel-Benhassine F, Bouziat R, Brandler S, Schwartz O, Moris A. The antiviral factor APOBEC3G improves CTL recognition of cultured HIV-infected T cells. *The Journal of experimental medicine.* 2010;207(1):39-49. doi:10.1084/jem.20091933.
62. Russell RA, Moore MD, Hu WS, Pathak VK. APOBEC3G induces a hypermutation gradient: purifying selection at multiple steps during HIV-1 replication results in levels of G-to-A mutations that are high in DNA, intermediate in cellular viral RNA, and low in virion RNA. *Retrovirology.* 2009;6:16. doi:10.1186/1742-4690-6-16.
63. Wang T, Zhang W, Tian C, Liu B, Yu Y, Ding L et al. Distinct viral determinants for the packaging of human cytidine deaminases APOBEC3G and APOBEC3C. *Virology.* 2008;377(1):71-9. doi:10.1016/j.virol.2008.04.012.
64. Friew YN, Boyko V, Hu WS, Pathak VK. Intracellular interactions between APOBEC3G, RNA, and HIV-1 Gag: APOBEC3G multimerization is dependent on its association with RNA. *Retrovirology.* 2009;6:56. doi:10.1186/1742-4690-6-56.
65. Desimmie BA, Delviks-Frankenberry KA, Burdick RC, Qi D, Izumi T, Pathak VK. Multiple APOBEC3 restriction factors for HIV-1 and one Vif to rule them all. *Journal of molecular biology.* 2014;426(6):1220-45. doi:10.1016/j.jmb.2013.10.033.

66. Feng Y, Baig TT, Love RP, Chelico L. Suppression of APOBEC3-mediated restriction of HIV-1 by Vif. *Frontiers in microbiology*. 2014;5:450. doi:10.3389/fmicb.2014.00450.
67. Sheehy AM, Gaddis NC, Malim MH. The antiretroviral enzyme APOBEC3G is degraded by the proteasome in response to HIV-1 Vif. *Nature medicine*. 2003;9(11):1404-7. doi:10.1038/nm945.
68. Jern P, Russell RA, Pathak VK, Coffin JM. Likely role of APOBEC3G-mediated G-to-A mutations in HIV-1 evolution and drug resistance. *PLoS pathogens*. 2009;5(4):e1000367. doi:10.1371/journal.ppat.1000367.
69. Kim EY, Lorenzo-Redondo R, Little SJ, Chung YS, Phalora PK, Maljkovic Berry I et al. Human APOBEC3 induced mutation of human immunodeficiency virus type-1 contributes to adaptation and evolution in natural infection. *PLoS pathogens*. 2014;10(7):e1004281. doi:10.1371/journal.ppat.1004281.
70. Goujon C, Moncorge O, Bauby H, Doyle T, Ward CC, Schaller T et al. Human MX2 is an interferon-induced post-entry inhibitor of HIV-1 infection. *Nature*. 2013;502(7472):559-62. doi:10.1038/nature12542. One of the three major papers released in 2013 first describing MX2 as an ISG that is also a restriction factor.
71. Kane M, Yadav SS, Bitzegeio J, Kutluay SB, Zang T, Wilson SJ et al. MX2 is an interferon-induced inhibitor of HIV-1 infection. *Nature*. 2013;502(7472):563-6. doi:10.1038/nature12653. One of the three major papers released in 2013 first describing MX2 as an ISG that is also a restriction factor.
72. Liu Z, Pan Q, Ding S, Qian J, Xu F, Zhou J et al. The interferon-inducible MxB protein inhibits HIV-1 infection. *Cell host & microbe*. 2013;14(4):398-410. doi:10.1016/j.chom.2013.08.015.

One of the three major papers released in 2013 first describing MX2 as an ISG that is also a restriction factor.

73. Fricke T, White TE, Schulte B, de Souza Aranha Vieira DA, Dharan A, Campbell EM et al. MxB binds to the HIV-1 core and prevents the uncoating process of HIV-1. *Retrovirology*. 2014;11:68. doi:10.1186/s12977-014-0068-x

10.1186/PREACCEPT-6453674081373986.

74. Liu Z, Pan Q, Liang Z, Qiao W, Cen S, Liang C. The highly polymorphic cyclophilin A-binding loop in HIV-1 capsid modulates viral resistance to MxB. *Retrovirology*. 2015;12:1. doi:10.1186/s12977-014-0129-1.

75. Matreyek KA, Wang W, Serrao E, Singh PK, Levin HL, Engelman A. Host and viral determinants for MxB restriction of HIV-1 infection. *Retrovirology*. 2014;11:90. doi:10.1186/s12977-014-0090-z.

76. Mavrommatis E, Fish EN, Platanias LC. The schlafen family of proteins and their regulation by interferons. *Journal of interferon & cytokine research : the official journal of the International Society for Interferon and Cytokine Research*. 2013;33(4):206-10. doi:10.1089/jir.2012.0133.

77. Li M, Kao E, Gao X, Sandig H, Limmer K, Pavon-Eternod M et al. Codon-usage-based inhibition of HIV protein synthesis by human schlafen 11. *Nature*. 2012;491(7422):125-8. doi:10.1038/nature11433.

78. Abdel-Mohsen M, Raposo RA, Deng X, Li M, Liegler T, Sinclair E et al. Expression profile of host restriction factors in HIV-1 elite controllers. *Retrovirology*. 2013;10:106. doi:10.1186/1742-4690-10-106.

79. Tada T, Zhang Y, Koyama T, Tobiume M, Tsunetsugu-Yokota Y, Yamaoka S et al. MARCH8 inhibits HIV-1 infection by reducing virion incorporation of envelope glycoproteins. *Nature medicine*. 2015;21(12):1502-7. doi:10.1038/nm.3956. *A study demonstrating how MARCH8 inhibits HIV-1 replication in macrophages by limiting envelopes incorporation into budding virions.*
80. Neil SJ, Zang T, Bieniasz PD. Tetherin inhibits retrovirus release and is antagonized by HIV-1 Vpu. *Nature*. 2008;451(7177):425-30. doi:10.1038/nature06553.
81. Kupzig S, Korolchuk V, Rollason R, Sugden A, Wilde A, Banting G. Bst-2/HM1.24 is a raft-associated apical membrane protein with an unusual topology. *Traffic*. 2003;4(10):694-709.
82. Perez-Caballero D, Zang T, Ebrahimi A, McNatt MW, Gregory DA, Johnson MC et al. Tetherin inhibits HIV-1 release by directly tethering virions to cells. *Cell*. 2009;139(3):499-511. doi:10.1016/j.cell.2009.08.039.
83. Galao RP, Le Tortorec A, Pickering S, Kueck T, Neil SJ. Innate sensing of HIV-1 assembly by Tetherin induces NFkappaB-dependent proinflammatory responses. *Cell host & microbe*. 2012;12(5):633-44. doi:10.1016/j.chom.2012.10.007.
84. Tokarev A, Suarez M, Kwan W, Fitzpatrick K, Singh R, Guatelli J. Stimulation of NF-kappaB activity by the HIV restriction factor BST2. *Journal of virology*. 2013;87(4):2046-57. doi:10.1128/JVI.02272-12.
85. Jia B, Serra-Moreno R, Neidermyer W, Rahmberg A, Mackey J, Fofana IB et al. Species-specific activity of SIV Nef and HIV-1 Vpu in overcoming restriction by tetherin/BST2. *PLoS pathogens*. 2009;5(5):e1000429. doi:10.1371/journal.ppat.1000429.

86. Kluge SF, Mack K, Iyer SS, Pujol FM, Heigele A, Learn GH et al. Nef proteins of epidemic HIV-1 group O strains antagonize human tetherin. *Cell host & microbe*. 2014;16(5):639-50. doi:10.1016/j.chom.2014.10.002.
87. Serra-Moreno R, Evans DT. Adaptation of human and simian immunodeficiency viruses for resistance to tetherin/BST-2. *Current HIV research*. 2012;10(4):277-82.
88. Dube M, Roy BB, Guiot-Guillain P, Mercier J, Binette J, Leung G et al. Suppression of Tetherin-restricting activity upon human immunodeficiency virus type 1 particle release correlates with localization of Vpu in the trans-Golgi network. *Journal of virology*. 2009;83(9):4574-90. doi:10.1128/JVI.01800-08.
89. McNatt MW, Zang T, Bieniasz PD. Vpu binds directly to tetherin and displaces it from nascent virions. *PLoS pathogens*. 2013;9(4):e1003299. doi:10.1371/journal.ppat.1003299.
90. Usami Y, Wu Y, Gottlinger HG. SERINC3 and SERINC5 restrict HIV-1 infectivity and are counteracted by Nef. *Nature*. 2015;526(7572):218-23. doi:10.1038/nature15400. *One of the first papers published on SERINC3/5 and how it restricts HIV-1 and is antagonized by nef.*
91. Inuzuka M, Hayakawa M, Ingi T. Serinc, an activity-regulated protein family, incorporates serine into membrane lipid synthesis. *The Journal of biological chemistry*. 2005;280(42):35776-83. doi:10.1074/jbc.M505712200.
92. Asmuth DM, Murphy RL, Rosenkranz SL, Lertora JJ, Kottlilil S, Cramer Y et al. Safety, tolerability, and mechanisms of antiretroviral activity of pegylated interferon Alfa-2a in HIV-1-monoinfected participants: a phase II clinical trial. *The Journal of infectious diseases*. 2010;201(11):1686-96. doi:10.1086/652420.

93. Adamson, C. S., & Freed, E. O. (2009). Anti-HIV-1 Therapeutics: From FDA-approved Drugs to Hypothetical Future Targets. *Molecular Interventions*, 9(2), 70–74.
<http://doi.org/10.1124/mi.9.2.5>
94. Smithgall, T. E., & Thomas, G. (2013). Small molecule inhibitors of the HIV-1 virulence factor, Nef. *Drug Discovery Today. Technologies*, 10(4), e451–e548.
<http://doi.org/10.1016/j.ddtec.2013.07.002>
95. Mohd Hanafiah K, Groeger J, Flaxman AD, Wiersma ST. Global epidemiology of hepatitis C virus infection:new estimates of age-specific antibody to HCV seroprevalence. *Hepatology*. 2013; 57(4):1333–42. doi: 10.1002/hep.26141 PMID: 23172780.
95. Mohd Hanafiah K, Groeger J, Flaxman AD, Wiersma ST. Global epidemiology of hepatitis C virus infection:new estimates of age-specific antibody to HCV seroprevalence. *Hepatology*. 2013; 57(4):1333–42. doi: 10.1002/hep.26141
96. Gravitz L. Introduction: a smouldering public-health crisis. *Nature*. 2011; 474(7350):S2–4. Epub 2011/07/20. doi: 10.1038/474S2a
97. Holmberg SD, Spradling PR, Moorman AC, Denniston MM. Hepatitis C in the United States. *N Engl J Med*. 2013; 368(20):1859–61. Epub 2013/05/17. doi: 10.1056/NEJMp1302973
98. Freeman ZT, Cox AL (2016) Lessons from Nature: Understanding Immunity to HCV to Guide Vaccine Design. *PLoS Pathog* 12(6): e1005632. doi:10.1371/journal.ppat.1005632
99. Osburn WO, Fisher BE, Dowd KA, Urban G, Liu L, Ray SC, et al. Spontaneous Control of Primary Hepatitis C Virus Infection and Immunity Against Persistent Reinfection. *Gastroenterology*. 2010; 138:315–24. S0016-5085(09)01658-8 [pii]; doi: 10.1053/j.gastro.2009.09.017 PubMed Central PMCID:PMC2889495.

100. Lanford RE, Guerra B, Chavez D, Bigger C, Brasky KM, Wang XH, et al. Cross-genotype immunity to hepatitis C virus. *J Virol.* 2004; 78:1575–81
101. Cooper S, Erickson AL, Adams EJ, Kansopon J, Weiner AJ, Chien DY, Houghton M, Parham P, Walker CM. Analysis of a successful immune response against hepatitis C virus. *Immunity.* 1999;Vol. 10(No. 4):439–449
102. Gruner NH, Gerlach TJ, Jung MC, Diepolder HM, Schirren CA, Schraut WW, Hoffmann R, Zachoval R, Santantonio T, Cucchiaroni M, Cerny A, Pape GR. Association of hepatitis C virusspecific CD8+ T cells with viral clearance in acute hepatitis C. *Journal of Infectious Diseases* 2000;Vol. 181(No. 5):1528–1536
103. Lechner F, Wong DK, Dunbar PR, Chapman R, Chung RT, Dohrenwend P, Robbins G, Phillips R, Klenerman P, Walker BD. Analysis of successful immune responses in persons infected with hepatitis C virus. *J.Exp.Med* 2000;Vol. 191(No. 9):1499–1512]
104. Takaki A, Wiese M, Maertens G, Depla E, Seifert U, Liebetrau A, Miller JL, Manns MP, Rehermann B. Cellular immune responses persist and humoral responses decrease two decades after recovery from a single-source outbreak of hepatitis C. *Nat.Med* 2000;Vol. 6(No. 5):578-582
105. Hiroishi K, Kita H, Kojima M, Okamoto H, Moriyama T, Kaneko T, Ishikawa T, Ohnishi S, Aikawa T, Tanaka N, Yazaki Y, Mitamura K, Imawari M. Cytotoxic T lymphocyte response and viral load in hepatitis C virus infection. *Hepatology* 1997;Vol. 25(No. 3):705–712
106. Rehermann B, Chang KM, McHutchison JG, Kokka R, Houghton M, Chisari FV. Quantitative analysis of the peripheral blood cytotoxic T lymphocyte response in patients with chronic hepatitis C virus infection. *Journal of Clinical Investigation* 1996;Vol. 98(No. 6):1432–1440

107. Cerny A, McHutchison JG, Pasquinelli C, Brown ME, Brothers MA, Grabscheid B, Fowler P, Houghton M, Chisari FV. Cytotoxic T lymphocyte response to hepatitis C virus-derived peptides containing the HLA A2.1 binding motif. *J. Clin. Invest* 1995; Vol. 95(No. 2):521–530
108. He XS, Rehermann B, Lopez-Labrador FX, Boisvert J, Cheung R, Mumm J, Wedemeyer H, Berenguer M, Wright TL, Davis MM, Greenberg HB. Quantitative analysis of hepatitis C virus specific CD8(+) T cells in peripheral blood and liver using peptide-MHC tetramers. *Proceedings of the National Academy of Sciences of the United States of America* 1999; Vol. 96(No. 10):5692–5697
109. Shirai M, Okada H, Nishioka M, Akatsuka T, Wychowski C, Houghton R, Pendleton CD, Feinstone SM, Berzofsky JA. An epitope in hepatitis C virus core region recognized by cytotoxic T cells in mice and humans. *Journal of Virology* 1994; Vol. 68(No. 5):3334–3342
110. Battegay M, Fikes J, Di Bisceglie AM, Wentworth PA, Sette A, Celis E, Ching W-M, Grakoui A, Rice CM, Kurokohchi K, Berzofsky JA, Hoofnagle JH, Feinstone SM, Akatsuka T. Patients with chronic hepatitis C have circulating cytotoxic T cells which recognize hepatitis C virus-encoded peptides binding to HLA-A2.1 molecules. *Journal of Virology* 1995; Vol. 69:2462–2470
111. Shoukry NH, Grakoui A, Houghton M, Chien DY, Ghayeb J, Reimann KA, Walker CM. Memory CD8+ T cells are required for protection from persistent hepatitis C virus infection. *Journal of Experimental Medicine* 2003; Vol. 197(No. 12):1645–1655
112. Thimme R, Oldach D, Chang KM, Steiger C, Ray SC, Chisari FV. Determinants of viral clearance and persistence during acute hepatitis C virus infection. *Journal of Experimental Medicine* 2001; Vol. 194(No. 10):1395–1406

113. Schulze zur Wiesch J, Ciuffreda D, Lewis-Ximenez L, Kasprovicz V, Nolan BE, Streeck H, et al. Broadly directed virus-specific CD4+ T cell responses are primed during acute hepatitis C infection, but rapidly disappear from human blood with viral persistence. *JExpMed*. 2012; 209:61–75. [pii]; doi: 10.1084/jem.20100388
114. Burke KP and Cox AL. Hepatitis C Virus Evasion of Adaptive Immune Responses- A Model for viral persistence. *Immunol Res*. 2010 July ; 47(1-3): 216–227. doi:10.1007/s12026-009-8152-3.
115. Eckels DD, Wang H, Bian TH, Tabatabai N, Gill JC. Immunobiology of hepatitis C virus (HCV) infection: the role of CD4 T cells in HCV infection. *Immunol.Rev* 2000;Vol. 174:90–97
116. Chang KM, Rehermann B, McHutchison JG, Pasquinelli C, Southwood S, Sette A, Chisari FV. Immunological significance of cytotoxic T lymphocyte epitope variants in patients chronically infected by the hepatitis C virus. *Journal of Clinical Investigation* 1997;Vol. 100(No. 9):2376–2385
117. Allen TM, Altfeld M, Yu XG, O'Sullivan KM, Lichtenfeld M, Le Gall S, John M, Mothe BR, Lee PK, Kalife ET, Cohen DE, Freedberg KA, Strick DA, Johnston MN, Sette A, Rosenberg ES, Mallal SA, Goulder PJ, Brander C, Walker BD. Selection, transmission, and reversion of an antigen-processing cytotoxic T-lymphocyte escape mutation in human immunodeficiency virus type 1 infection. *Journal of Virology* 2004;Vol. 78(No. 13):7069–7078
118. Timm J, Lauer GM, Kavanagh DG, Sheridan I, Kim AY, Lucas M, Pillay T, Ouchi K, Reyor LL, Zur Wiesch JS, Gandhi RT, Chung RT, Bhardwaj N, Klenerman P, Walker BD, Allen TM. CD8 epitope escape and reversion in acute HCV infection. *Journal of Experimental Medicine* 2004;Vol. 200(No. 12):1593–1604

119. Kimura Y, Gushima T, Rawale S, Kaumaya P, Walker CM. Escape mutations alter proteasome processing of major histocompatibility complex class I-restricted epitopes in persistent hepatitis C virus infection. *J Virol* 2005;Vol. 79(No. 8):4870–4876
120. Seifert U, Liermann H, Racanelli V, Halenius A, Wiese M, Wedemeyer H, Ruppert T, Rispetter K, Henklein P, Sijts A, Hengel H, Kloetzel PM, Rehermann B. Hepatitis C virus mutation affects proteasomal epitope processing. *J.Clin.Invest* 2004;Vol. 114(No. 2):250–259
121. Allen TM, O'Connor DH, Jing P, Dzuris JL, Mothe BR, Vogel TU, Dunphy E, Liebl ME, Emerson C, Wilson N, Kunstman KJ, Wang X, Allison DB, Hughes AL, Desrosiers RC, Altman JD, Wolinsky SM, Sette A, Watkins DI. Tat-specific cytotoxic T lymphocytes select for SIV escape variants during resolution of primary viraemia. *Nature* 2000;Vol. 407(No. 6802):386–390
122. Jones NA, Wei X, Flower DR, Wong M, Michor F, Saag MS, Hahn BH, Nowak MA, Shaw GM, Borrow P. Determinants of human immunodeficiency virus type 1 escape from the primary CD8+cytotoxic T lymphocyte response. *Journal of Experimental Medicine* 2004;Vol. 200(No. 10):1243–1256
123. Cox, Andrea & Mosbrugger, Timothy & Mao, Qing & Liu, Zhi & Wang, Xiao-Hong & Yang, Hung-Chih & Sidney, John & Sette, Alessandro & Pardoll, Drew & Thomas, David & Ray, Stuart. (2005). Cellular immune selection with hepatitis C virus persistence in humans. *The Journal of experimental medicine*. 201. 1741-52. 10.1084/jem.20050121.
124. Yokomaku Y, Miura H, Tomiyama H, Kawana-Tachikawa A, Takiguchi M, Kojima A, Nagai Y, Iwamoto A, Matsuda Z, Ariyoshi K. Impaired processing and presentation of cytotoxic-Tlymphocyte (CTL) epitopes are major escape mechanisms from CTL immune pressure in human immunodeficiency virus type 1 infection. *J Virol* 2004;Vol. 78(No. 3):1324–1332

125. Rutebemberwa A, Ray SC, Astemborski J, Levine J, Liu L, Dowd KA, Clute S, Wang C, Korman A, Sette A, Sidney J, Pardoll DM, Cox AL. High-programmed death-1 levels on hepatitis C virus- specific T cells during acute infection are associated with viral persistence and require preservation of cognate antigen during chronic infection. *Journal of Immunology* 2008;Vol. 181(No. 12):8215–8225.
126. Barber DL, Wherry EJ, Masopust D, Zhu B, Allison JP, Sharpe AH, Freeman GJ, Ahmed R. Restoring function in exhausted CD8 T cells during chronic viral infection. *Nature* 2006;Vol. 439(No. 7077):682–687
127. Goldberg MV, Maris CH, Hipkiss EL, Flies AS, Zhen L, Tudor RM, Grosso JF, Getnet D, Whartenby KA, Brockstedt DG, Dubensky TW Jr, Chen L, Pardoll DM, Drake CG. Role of PD-1 and its ligand, B7-H1, in early fate decisions of CD8 T cells. *Blood*. 2007
128. Azzoni L, Foulkes AS, Pappasavvas E, Mexas AM, Lynn KM, Mounzer K, et al. Pegylated Interferon alfa-2a monotherapy results in suppression of HIV type 1 replication and decreased cell-associated HIV DNA integration. *J Infect Dis*. 2013;207: 213–222. doi:10.1093/infdis/jis663
129. El-Diwany, R., Soliman, MG, Sugawara, S. et al., CMPK2 and BCL-G are associated with type 1 interferon-induced HIV restriction in humans. *Sci Adv*, 2018. 4(8): p. eaat0843.
130. Y. Xu, M. Johansson, A. Karlsson, Human UMP-CMP kinase 2, a novel nucleoside monophosphate kinase localized in mitochondria. *J. Biol. Chem*. 283, 1563–1571 (2008).
131. A. F. Weil, D. Ghosh, Y. Zhou, L. Seiple, M. A. McMahon, A. M. Spivak, R. F. Siliciano, J. T. Stivers, Uracil DNA glycosylase initiates degradation of HIV-1 cDNA containing misincorporated dUTP and prevents viral integration. *Proc. Natl. Acad. Sci. U.S.A.* 110, E448–E457 (2013).

132. B. Guo, A. Godzik, J. C. Reed, Bcl-G, a novel pro-apoptotic member of the Bcl-2 family. *J. Biol. Chem.* 276, 2780–2785 (2001).
133. Luo, Na & Wu, Yi & Chen, Yongwen & Yang, Zhao & Guo, Sheng & Fei, Lei & Zhou, Di & Yang, Chengying & Wu, Shengxi & Ni, Bing & Hao, Fei & Wu, Yuzhang. (2009). Upregulated BclGL expression enhances apoptosis of peripheral blood CD4+ T lymphocytes in patients with systemic lupus erythematosus. *Clinical immunology (Orlando, Fla.)*. 132. 349-61.
10.1016/j.clim.2009.05.010.
134. Hochberg Y, Benjamini Y. More powerful procedures for multiple significance testing. *Stat Med.* 1990;9: 811–818.
135. Vandergeeten, Claire & Fromentin, Rémi & Merlini, Esther & Bramah-Lawani, Mariam & Dafonseca, Sandrina & Bakeman, Wendy & McNulty, Amanda & Ramgopal, Moti & Michael, Nelson & Kim, Jerome & Ananworanich, Jintanat & Chomont, Nicolas. (2014). Cross-clade Ultrasensitive PCR-based Assays to Measure HIV Persistence in Large Cohort Studies.. *Journal of virology*. 88. 10.1128/JVI.00609-14.
136. Goujon C, Malim MH. Characterization of the alpha interferon-induced postentry block to HIV-1 infection in primary human macrophages and T cells. *J Virol.* 2010;84:9254–9266
137. Shan, Liang & Rabi, S Alireza & Laird, Gregory & Eisele, Evelyn & Zhang, Hao & Margolick, Joseph & Siliciano, Robert. (2013). A novel PCR assay for quantification of HIV-1 RNA. *Journal of virology*. 87. 10.1128/JVI.00006-13.
138. Eldeeb, Mohamed & Fahlman, Richard & Esmaili, Mansoor & Ragheb, Mohamed. (2018). Regulating Apoptosis by Degradation: The N-End Rule-Mediated Regulation of Apoptotic

- Proteolytic Fragments in Mammalian Cells. *International Journal of Molecular Sciences*. 19. 3414. 10.3390/ijms19113414.
139. Giam M, Okamoto T, Mintern JD, Strasser A, Bouillet P. Bcl-2 family member Bcl-G is not a proapoptotic protein. *Cell Death Dis*. 2012;3: e404. doi:10.1038/cddis.2012.130
140. Follis, Ariele & Llambi, Fabien & Kalkavan, Halime & Yao, Yong & Phillips, Aaron & Park, Cheon-Gil & Marassi, Francesca & Green, Douglas & Kriwacki, Richard. (2018). Regulation of apoptosis by an intrinsically disordered region of Bcl-xL. *Nature Chemical Biology*. 14. 1. 10.1038/s41589-018-0011-x.
141. Chinnaiyan, Arul & Hanna, William & Orth, Kim & Duan, Hangjun & Poirier, Guy & Froelich, Christopher & Dixit, Vishva. (1996). Cytotoxic T-cell-derived granzyme B activates the apoptotic protease ICE-LAP3. *Current biology : CB*. 6. 897-9. 10.1016/S0960-9822(02)00614-0.
142. Manches, Olivier & Bhardwaj, Nina. (2009). Resolution of immune activation defines nonpathogenic SIV infection. *The Journal of clinical investigation*. 119. 3512-5. 10.1172/JCI41509.
143. Chandrasekar, Aswath & Cummins, Nathan & Badley, Andrew. (2019). The Role of the BCL-2 Family of Proteins in HIV-1 Pathogenesis and Persistence. *Clinical Microbiology Reviews*. 33. 10.1128/CMR.00107-19.
144. Miled, Chaouki & Pontoglio, Marco & Garbay, Serge & Yaniv, Moshe & Weitzman, Jonathan. (2005). A Genomic Map of p53 Binding Sites Identifies Novel p53 Targets Involved in an Apoptotic Network. *Cancer research*. 65. 5096-104. 10.1158/0008-5472.CAN-04-4232.

145. Thimme R, Bukh J, Spangenberg HC, Wieland S, Pemberton J, Steiger C, et al. Viral and immunological determinants of hepatitis C virus clearance, persistence, and disease. *Proc Natl Acad Sci U S A* (2002) 99(24):15661–8. doi:10.1073/pnas.202608299
146. Major ME, Dahari H, Mihalik K, Puig M, Rice CM, Neumann AU, et al. Hepatitis C virus kinetics and host responses associated with disease and outcome of infection in chimpanzees. *Hepatology* (2004) 39(6):1709–20. doi:10.1002/hep.20239
147. Diepolder HM, Zachoval R, Hoffmann RM, Wierenga EA, Santantonio T, Jung MC, et al. Possible mechanism involving T-lymphocyte response to non-structural protein 3 in viral clearance in acute hepatitis C virus infection. *Lancet* (1995) 346(8981):1006–7. doi:10.1016/S0140-6736(95)91691-1
148. Golden-Mason L, Palmer B, Klarquist J, Mengshol JA, Castelblanco N, Rosen HR. Upregulation of PD-1 expression on circulating and intrahepatic hepatitis C virus-specific CD8+ T cells associated with reversible immune dysfunction. *J Virol* (2007) 81(17):9249–58. doi:10.1128/JVI.00409-07
149. Nakamoto N, Cho H, Shaked A, Olthoff K, Valiga ME, Kaminski M, et al. Synergistic reversal of intrahepatic HCV-specific CD8 T cell exhaustion by combined PD-1/CTLA-4 blockade. *PLoS Pathog* (2009) 5(2):e1000313. doi:10.1371/journal.ppat.1000313
150. Nakamoto N, Kaplan DE, Coleclough J, Li Y, Valiga ME, Kaminski M, et al. Functional restoration of HCV-specific CD8 T cells by PD-1 blockade is defined by PD-1 expression and compartmentalization. *Gastroenterology* (2008) 134(7):1927–37. doi:10.1053/j.gastro.2008.02.033

151. Golden-Mason L, Palmer BE, Kassam N, Townshend-Bulson L, Livingston S, McMahon BJ, et al. Negative immune regulator Tim-3 is overexpressed on T cells in hepatitis C virus infection and its blockade rescues dysfunctional CD4+ and CD8+ T cells. *J Virol* (2009) 83(18):9122–30. doi:10.1128/JVI.00639-09
152. McMahan RH, Golden-Mason L, Nishimura MI, McMahon BJ, Kemper M, Allen TM, et al. Tim-3 expression on PD-1+ HCV-specific human CTLs is associated with viral persistence, and its blockade restores hepatocyte-directed in vitro cytotoxicity. *J Clin Invest* (2010) 120(12):4546–57. doi:10.1172/JCI43127
153. Cox A, Netski D, Mosbruger T, et al. Prospective evaluation of community-acquired acute-phase hepatitis C virus infection. *Clin Infect Dis*. 2005;40:951–8
154. Cox AL, Mosbruger T, Lauer GM, et al. Comprehensive analyses of CD8+ T cell responses during longitudinal study of acute human hepatitis C. *Hepatology*. 2005;42:104–12
155. Bengsch B, Seigel B, Ruhl M, Timm J, Kuntz M, Blum HE, et al. Coexpression of PD-1, 2B4, CD160 and KLRG1 on exhausted HCV-specific CD8+ T cells is linked to antigen recognition and T cell differentiation. *PLoS Pathogen* (2010) 6(6) :e1000947.10.1371/ journal. ppat. 1000947
156. Kaech SM, Tan JT, Wherry EJ, Konieczny BT, Surh CD, Ahmed R. Selective expression of the interleukin 7 receptor identifies effector CD8 T cells that give rise to long-lived memory cells. *Nat Immunol* (2003) 4(12):1191–810.1038/ni1009
157. Wieland, Dominik & Kemming, Janine & Schuch, Anita & Emmerich, Florian & Knolle, Percy & Neumann-Haefelin, Christoph & Held, Werner & Zehn, Dietmar & Hofmann, Maike & Thimme, Robert. (2017). TCF1+ hepatitis C virus-specific CD8+ T cells are maintained after

cessation of chronic antigen stimulation. Nature Communications. 8. 15050.

10.1038/ncomms15050.

Curriculum Vitae

Mary Soliman

E-Mail: msolima5@jhmi.edu

Education

Ph.D, Cellular and Molecular Medicine **August 2014-August 2020**
Johns Hopkins Medical Institute

Bachelor of Science, Biology **August 2010-June 2014**
University of California, Irvine

Experience

Johns Hopkins University School of Medicine Graduate School Research **2014-Ongoing**
Andrea Cox, M.D. Ph.D and Ashwin Balagopal, M.D.

- Project 1: The longitudinal study of T cell responses (phenotypically and functionally) in HCV monoinfected individuals who naturally clear infection multiple times compared to those who remain chronically infected.
- Project 2: The study of BCL-G as an interferon stimulated gene that restricts HIV-1 replication.

Undergraduate Biomedical Research

Dr. Luis Mota-Bravo University of California, Irvine **Spring 2012**

- Assess the relationship between common local sources of water (ie. soda dispensers, bathrooms, reservoirs) and antibiotic resistance compared to those in a clinical setting.

Dr. Brian Stramer, King's College London, UK **Summer 2012**

- Study the role of contact inhibition of locomotion in hemocyte disturbance in *Drosophila* flies.

Dr. Young Jik Kwon University of California, Irvine **Fall 2012-Spring 2014**

- Synthesizing protamine-sulfate nano-particles in order to enter into dendritic based cell lines.

Grants and Fellowships

NIH-Minority Access to Research Careers (MARC) **2012-2014**
NIH-Minority Biomedical Research Support Program (MBRS) for Undergraduates **Spring 2012**
NIH-Minority Health and Health Disparities International Research Training **Summer 2012**

Honors and Awards

Member of Pre-Health National Honors Society: Phi Delta Epsilon **2013-2014**
First place prize for Cellular and Molecular Medicine 3 Minute Thesis Competition **2018**
Member of Montgomery County Women's Democratic Club **2019-ongoing**

Publications

- Bruner KM, Murray AJ, Pollack RA, **Soliman MG**, Laskey SB, Capoferri AA, Lai J, Strain MC, Lada SM, Hoh R, Ho YC, Richman DD, Deeks SG, Siliciano JD, Siliciano RF. Defective proviruses rapidly accumulate during acute HIV-1 infection. Nat Med. 2016 Aug 8. PMID:27500724
- **Mary Soliman**, Geetha Srikrishna, Ashwin Balagopal. MECHANISMS OF HIV CONTROL. HIV/AIDS Current Opinions. Curr HIV/AIDS Rep. 2017 June
- Ramy El-Diwany, Florian Breitwieser, **Mary Soliman**, Alyza Skaist, Geetha Srikrishna, Robert F. Siliciano, Joel N. Blankson, Stuart C. Ray, Steven Salzberg, Sarah Wheelan, David L. Thomas, Ashwin Balagopal. HIV-1 Transcription and CD4+ T cell Activation in Patients Starting Antiretrovirals. AIDS. 2017 June
- Ramy El-Diwany, **Mary Soliman**, Sho Sugawara, Florian Breitwieser, Alyza Skaist, Candelaria Coggiano, Neel Sangal, Michael Chattergoon, Justin R. Bailey, Robert F. Siliciano, Joel N. Blankson, Stuart C. Ray, Sarah J. Wheelan, David L. Thomas, Ashwin Balagopal. CMPK2 and BCL-G are Interferon Induced Determinants of HIV Restriction in Humans. Science Advances 2018 August
- Kinchen VJ, Zahid MN, Flyak AI, **Soliman MG et al.** Broadly Neutralizing Antibody Mediated Clearance of Human Hepatitis C Virus Infection. Cell Host Microbe. 2018 November

Presentations

- **Soliman, Mary.** *Identification of CMPK2 as an Interferon Stimulated Gene that Restricts HIV Infection.* American Association of Immunologists (AAI) Conference. Washington, D.C., May 2017.
- **Soliman, Mary.** *Comprehensive Development of MALDI Imaging for Analysis of Peptides and Small Molecules in SIV Spleen.* American Association for the Advancement of Science (AAAS) Conference, Chicago, IL. February 2014.
- **Soliman, Mary.** *Comprehensive Development of MALDI Imaging.* Annual Biomedical Research Conference for Minority Students (ABRCMS), Nashville, TN. November 2013.
- **Soliman, Mary.** *Comprehensive Development of MALDI Imaging.* Leadership Alliance Conference. Stamford, CN. August 2013
- **Soliman, Mary.** *Development of a screening approach and novel tools to identify genes involved in Contact Inhibition of Locomotion.* American Association for the Advancement of Science (AAAS) Conference, Boston, MA. February 2013.
- **Soliman, Mary.** *Development of a screening approach and novel tools to identify genes involved in Contact Inhibition of Locomotion.* Annual Biomedical Research Conference for Minority Students (ABRCMS), San Jose, CA. 2012